 CMES, vol.19, no.1, pp.69-98, 2007

A Novel Form of Reproducing Kernel Interpolation Method with Applications to Nonlinear Mechanics

Amit Shaw[1] **and D Roy**[2]

Abstract: A novel discretization strategy and derivative reproduction based on reproducing kernel (RK) particle approximations of functions are proposed. The proposed scheme is in the form of an RK interpolation that offers significant numerical advantages over a recent version of the strategy by Chen et al. (2003), wherein the authors added a set of primitive functions to the reproducing kernel (enrichment) functions. It was also required that the support size of the primitive function be less than the smallest distance between two successive grid points. Since the primitive function was required to vary from 0 to 1 within half of this support size, this potentially led to considerable numerical corruption of the algorithm. In contrast, the present version of the interpolating strategy, which is far less prone to such numerical ill-conditioning, linearly combines two different families of RK basis functions and determines the coefficients of the linear combination using the interpolating conditions. Apart from the interpolation scheme, a new technique for approximating derivatives of RK basis functions is also proposed. Such an approximation is based on a direct reproduction of derivatives within any given polynomial space. Detailed error estimates are provided and convergence studies are performed for a couple of test boundary value problems with known exact solutions. The proposed method is next applied to a class of one-dimensional beam equations (Elastica and Plastica) and a two-dimensional von Karman plate equation. Some of these results are compared with those obtained from a few other competing algorithms, such as the standard form of RK particle method, the interpolating RK method by Chen et al. (2003) as well as the classical finite element method. The relative numerical advantages of the new method are brought out in the process.

[1] Research Scholar; Structures Lab, Department of Civil Engineering, Indian Institute of Science, Bangalore 560012, India.

[2] Associate Professor; Communicating author; Email: royd@civil.iisc.ernet.in; Structures Lab, Department of Civil Engineering, Indian Institute of Science, Bangalore 560012, India.

1 The Introduction

Recently the idea of mesh free methods for numerical solutions of partial differential equations (PDE-s) has found considerable appeal amongst researchers. These methods, unlike classical forms of finite element methods, do not require any mesh generation for discretizations of complicated structural geometries defined over 1, 2 or 3 dimensions. In the process, several mesh-free methods have been developed and reported over the last two decades. In particular, mention may be made of the diffuse element method (DEM) (Nayrole *et al*. 1992), the element free Galerkin method (EFG) (Belytschko *et al*. 1994, Barry and Saigal 1999, Kaljevic and Saigal 1997, Lu *et al*. 1994), the partition of unity finite element method (PUFEM) (Babuska and Melenk 1997, Melenk and Babuska 1996), the $h-p$ Clouds (Duarte and Oden 1997), the moving least-square reproducing kernel method (MLSRK) (Liu *et al*. 1995a, 1995b, Liu and Belytschko 1996, Chen *et al*. 1996, 1997, Jin et al. 2001, Atluri et al. 2002a, 2004a), the meshless local boundary integral equation method (LBIE) (Zhu *et al*. 1998), the smooth particle hydrodynamics method (Gingold and Monaghan 1977), the meshless local Petrov–Galerkin method (MLPG) (Atluri *et al*. 1998, 2002b, 1999), mesh-free point collocation methods (Aluru 2000), the point interpolation method (Liu and Gu, 1999, 2000b, 2001a, b, c, d), the boundary point interpolation methods (Liu

and Gu, 2000d; Gu and Liu 2001a, b), the reproducing kernel element method (Liu *et al*. 2004, Li *et al*. 2004, Lu *et al*. 2004, Simkins *et al*. 2004) and several others.

Mesh-free shape functions are generally not interpolating in most of the methods noted above and thus it is difficult to impose essential boundary conditions, to apply nodal loads and even to derive collocation methods towards obtaining strong solutions of the governing differential equations. As reported in the literature, interpolating properties in mesh-free approximation may be achieved in several ways - such as coupling of mesh-free and finite element shape functions with a ramping in the transition zone (Krongauz and Belytschko 1996), coupling and enrichment of finite element and mesh-free shape functions with reproducing conditions (Huerta and Fernandez-Mendez 2000), hierarchical enrichment of finite element solutions using a mesh-free approximation (Wagner and Liu 2001). All these methods require an underlying grid structure for construction of finite element shape functions. Based on the idea of coupling mesh-free and finite element shape function (Krongauz *et al*. 1996 and Huerta *et al*. 2000), Chen *et al.* (2003) have proposed a technique for mesh-free approximation that recovers nodal values at designated grid points without any finite element enrichment. This method of mesh-free approximation is constituted of a primitive function and an enrichment function. While the primitive function is used to introduce the Kronecker delta properties, the enrichment function is for imposing the polynomial reproducing conditions. However, to satisfy the Kronecker delta property, the support size of primitive functions is chosen sufficiently small so it does not cover (contain) any neighboring points. However, since the primitive function is constrained to achieve a value of unity within about half of this small support size (starting from zero at the support boundary), it is likely to cause ill-conditioning of the reduced (projected) system equations leading to spurious oscillations, especially in higher derivatives, in the approximated function(s).

The purpose of this paper is to propose and numerically explore a new form of mesh-free, interpolating functional approximations and their derivatives through the reproducing kernel approach. In the conventional form of the reproducing kernel particle method (RKPM), derivatives of the moment matrix and correction functions are required for the construction of derivatives of shape functions. This may potentially lead to considerable numerical errors and Gibbs' phenomena especially in the higher order derivatives. Therefore the development of efficient algorithm for derivative construction of meshfree shape functions is still an active research area. Many authors have addressed the issue of efficient approximations of derivatives of the meshless interpolation functions. A meshless finite volume method (MFVM) through MLPG mixed approach has been proposed and numerically explored by Atluri et al. (2004b, 2005, 2006a, 2006b), Han *et al*. (2005, 2006). In the MLPG mixed approach, both the displacement function and its derivatives (strains, velocity, displacement gradient etc.) are interpolated separately. Consequently, costly differentiations of meshfree shape functions at the quadrature points are avoided. In this study, a new scheme for approximating derivatives of RKPM basis functions is proposed. It is based on the premise that the β^{th} derivative of RKPM basis functions will exactly reproduce the β^h derivative of an arbitrary function in the space of polynomial P_p of degree $p \geq |\beta|$. This derivative reproduction scheme does not require computing derivatives of the moment matrix and correction functions. Moreover a novel and numerically stable interpolating scheme, which eases the treatment of essential boundary conditions and imposed nodal loads, is proposed in this paper. The first step in the derivation of the interpolating form is to make use of weighted B-splines as basis functions to approximate a smooth function. Weights are obtained from the polynomial reproducing conditions. Then another set of non-B-spline basis functions are used to obtain the requisite correction so that the entire approximation becomes interpolating. Owing to the variation diminishing property of B-spline curves, it can reproduce sharp layers very accurately. For constructing the correction function, an exponential window function has been used. An analysis of the order of

accuracy and convergence of the method is provided. The proposed algorithm is then applied for numerical studies of a few non-linear boundary value problems of typical interest in solid mechanics. In the process, it is numerically verified that the present version of the derivative reproduction and interpolating strategy has a higher numerical stability as compared with a few other competing algorithms, such as the standard form of RKPM and the interpolating RKPM proposed recently by Chen *et al*. (2003).

2 The Reproducing Kernel Approximation

For purposes of a better appreciation of the algorithms to be presented in the following sections, it is essential to briefly introduce the concept of functional approximation through RKPM. Let $u(x)$, $x \in R^n$ be a sufficiently smooth function defined on a simply connected open set $\Omega \subset R^n$ with Lipschitz continuous boundary and $P_p = P_p(\Omega)$ the vector space of the polynomials of degree $\leq p$ on Ω where p is the highest degree of polynomials that can be reproduced by the mesh-free shape functions. Dimension of P_p is $(p+n)!/p!n!$. For convenience multi-index notation is adopted throughout the paper. Thus, defining $\alpha = (\alpha_1, \alpha_2, \ldots\ldots \alpha_n)$ (with $n > 0$) to be an n-tuple of non-negative integersα_j, α is referred to as the multi-index and its length is defined as $|\alpha| = \sum_{i=1}^{n} \alpha_i$. Then α^{th} (Fréchet) derivative of function $u(x)$ can be expressed as $D^\alpha u(x) = \partial_{x_1}^{\alpha_1} \partial_{x_2}^{\alpha_2} \ldots\ldots \partial_{x_3}^{\alpha_n} u(x)$. Similarly $\alpha! = \alpha_1!\alpha_2!\ldots\ldots\alpha_n!$ and $x^\alpha = x_1^{\alpha_1} x_2^{\alpha_2} \ldots\ldots x_n^{\alpha_n}$. Let $\overline{\Omega} = \Omega \cup \partial\Omega$ be the (closed) domain of interest discretized by a set of grid points $\left\{ \{x_i\}_{i=1}^{N_P} \right\} \subset \overline{\Omega}$ (also referred to as particles) so that one can define the set of discretized function values $\left\{ u_i \stackrel{\Delta}{=} u(x_i) \right\}_{i=1}^{N_P}$. Then a continuous function $u(x) \in C(\Omega)$ may be approximated as:

$$u^a(x) = \sum_{i=1}^{N_P} C(x-x_i)\phi_{a_i}(x-x_i)u_i \tag{1}$$

where $a_i \in R^+$ is called the *dilation parameter* associated with i^{th} node (particle), $\left\{ \phi_i \stackrel{\Delta}{=} \phi(x-x_i) \right\}$ is a set of finitely and compactly supported basis functions centered at x_i, $\phi_a(x) = \phi(x/a)$ is the a-dilated basis function. $C(x-x_i)$ is presently referred to as the correction function and may expressed as:

$$C(x-x_i) = H^T(x-x_i)b(x) \tag{2}$$

where $H^T(x-x_i) = \{(x-x_i)^\alpha\}_{|\alpha|\leq p}$ is a set of monomial basis functions and $b(x) = \{b_\alpha(x)\}_{|\alpha|\leq p}$ are coefficient functions that may be interpreted as moving with the location of approximation x. Now equation (1) may be written as:

$$u^a(x) = \sum_{i=1}^{N_P} \Psi_i(x)u_i \tag{3}$$

$$\Psi_i(x) = H^T(x-x_i)b(x)\phi_{a_i}(x-x_i) \tag{4}$$

The coefficient function vector $b(x)$ is determined from the following polynomial reproducing conditions:

$$\sum_{i=1}^{N_P} \Psi_i(x)x_i^\alpha = x^\alpha, \quad |\alpha| \leq p \tag{5}$$

$$\Rightarrow \sum_{i=1}^{N_P} \Psi_i(x)(x-x_i)^\alpha = \delta_{|\alpha|,0}, \quad |\alpha| \leq p \tag{6}$$

$$\Rightarrow \sum_{i=1}^{N_P} H^T(x-x_i)\cdot b(x)\phi_{a_i}(x-x_i)H(x-x_i) = H(0) \tag{7}$$

$$\Rightarrow M(x)b(x) = H(0) \tag{8}$$

where,

$$b(x) = M^{-1}(x)H(0) \tag{9}$$

is the coefficient vector and

$$M(x) = \sum_{i=1}^{N_P} H(x-x_i)H^T(x-x_i)\phi_{a_i}(x-x_i) \tag{10}$$

is the moment matrix. Using equations (4) and (9), RKPM shape function $\Psi_i(x)$ may be expressed as:

$$\Psi_i(x) = H^T(0)M^{-1}(x)H(x-x_i)\phi_{a_i}(x-x_i) \tag{11}$$

Derivatives of RKPM shape functions, obtained form equation (11) may be determined as:

$$\Psi_{i,x_k} = C_{,x_k}\phi_{a_i} + C\phi_{a_i,x_k}, \quad k \in [1, N_P] \tag{12}$$

where $C_{,x_k}$ and ϕ_{a_i,x_k} are first derivatives of the correction function C and the kernel function ϕ_{a_i} respectively with respect to x_k. $C_{,x_k}$ may be calculated as:

$$C_{,x_k} = H_{,x_k} b(x) + H b_{,x_k} \tag{13}$$

where $b_{,x_k}(x)$ is the vector containing the x_k-derivative of the correction function coefficients and may be obtained from the reproducing conditions as:

$$M_{,x_k} b + M b_{,x_k} = 0 \tag{14}$$

where $M_{,x_k}$ is the first derivatives of moment matrix $M(x)$. Similarly second order derivative of $\Psi_i(x)$ may be obtained by the following set of equations:

$$M_{,x_k x_k} b + 2M_{,x_k} b_{,x_k} + M b_{,x_k x_k} = 0 \tag{15a}$$

$$\Rightarrow b_{,x_k x_k} = -M^{-1}(M_{,x_k x_k} b + 2M_{,x_k} b_{,x_k}) \tag{15b}$$

$$C_{,x_k} = H_{,x_k x_k} b + 2H_{,x_k} b_{,x_k} + H b_{,x_k x_k} \tag{15c}$$

$$\Psi_{i,x_k x_k} = C_{,x_k x_k}\phi_{a_i} + C_{,x_k}\phi_{a_i,x_k x_k} + C\phi_{a_i,x_k x_k} \tag{15d}$$

Still higher order derivatives of $\Psi_i(x)$ may be computed in a similar fashion. Since derivative construction in this manner requires derivatives of the moment matrix and correction functions, it is numerically intensive and may potentially lead to considerable numerical error especially in higher order derivatives. A way to circumvent this difficulty is proposed in the next section wherein derivatives of RKPM basis functions are shown to be computable based on the polynomial reproduction condition within a given finite-dimensional polynomial space.

3 A New Scheme for Derivative Reproductions

Numerically accurate and stable computation of derivatives plays an important role in the performance of a mesh-free collocation algorithm applied to solve any differential equation. A novel and numerically accurate scheme for computations of derivatives of RKPM basis functions is proposed in this section. It is based on the premise that α^{th} derivatives of RKPM basis functions will exactly reproduce α^{th} derivatives of an arbitrary element of the space P_p of polynomials of degree $p \geq |\alpha|$. Thus following Liu and Belytschko (1997), consistency relations for derivatives of RKPM basis functions for $\phi \in C^k(\Omega)$ are

$$\sum_{i=1}^{N_P} D^\beta \Psi_i(x)(x - x_i)^\alpha = (-1)^{|\beta|}\alpha!\delta_{\beta\alpha}, \quad \forall |\beta| \leq k, |\alpha| \leq p \tag{16}$$

Now, let $\Psi_i^{(\beta)}(x) \triangleq D^\beta \Psi_i(x)$ be another family of RKPM basis functions, which exactly reproduce β^{th} derivatives of elements in the space P_p for $p \geq |\alpha|$ and $\forall |\beta| \leq k$. Then equation (12) may be written as:

$$\sum_{i=1}^{N_P} \Psi_i^{(\beta)}(x)(x - x_i)^\alpha = (-1)^{|\beta|}\alpha!\delta_{\beta\alpha}, \quad \forall |\beta| \leq k, |\alpha| \leq p \tag{17}$$

$$\Rightarrow \sum_{i=1}^{N_P} \Psi_i^{(\beta)}(x) H(x - x_i) = (-1)^{|\beta|} H^{(\beta)}(0), \quad \forall |\beta| \leq k \tag{18}$$

where $H^{(\beta)}(x) \triangleq D^\beta H(x)$ be the β^{th} derivative of monomial basis function $H(x)$ and is given by:

$$H^{(\beta)}(x) = \left\{ \frac{\alpha!}{(\alpha - \beta)!} x^{\varepsilon_{\alpha\beta}} : \varepsilon_{\alpha\beta} = (\alpha - \beta) \text{ if } \beta \leq |\alpha| \text{ and } 0 \text{ if } \beta > |\alpha| \right\} \tag{19}$$

It is clear from equation (19) that$H^{(0)}(x) = H(x)$. For example, in the one-dimensional case $(n = 1)$, one has:

$$H^{(0)} = H(x) = \{1,\ x,\ x^2,\ x^3 \ldots\ldots x^p\} \tag{20a}$$

$$H^{(1)} = \{0,\ 1,\ 2x,\ 3x^2 \ldots\ldots p x^{p-1}\} \tag{20b}$$

$$H^{(2)} = \{0,\ 0,\ 2,\ 6x \ldots\ldots p(p-1)x^{p-2}\} \tag{20c}$$

$\Psi_i^{(\beta)}(x)$ may be constructed in the same way as the RKPM basis functions. Now equation (18) may be written as:

$$\sum_{i=1}^{N_P} C^{\beta}(x-x_i)\phi_{a_i}(x-x_i)H(x-x_i) = (-1)^{|\beta|}H^{(\beta)}(0) \quad (21)$$

where $\Psi_i^{(\beta)} = C^{\beta}(x-x_i)\phi_{a_i}(x-x_i)$ (22)

$$\sum_{i=1}^{N_P} H^T(x-x_i)b^{\beta}(x)\phi_{a_i}(x-x_i)H(x-x_i) = (-1)^{|\beta|}H^{(\beta)}(0) \quad (23)$$

where $C^{\beta}(x-x_i) = H^T(x-x_i)b^{\beta}(x)$ is the correction function for the β^{th} derivative reproduction and $b^{\beta}(x) = \{b_{\alpha}^{\beta}(x)\}_{|\alpha|\leq p}$ is the vector of unknown coefficients. Equation (23) may now be written as:

$$M(x)b^{\beta}(x) = (-1)^{|\beta|}H^{(\beta)}(0) \quad (24)$$

$$\Rightarrow b^{\beta}(x) = (-1)^{|\beta|}M^{-1}(x)H^{(\beta)}(0) \quad (25)$$

From equations (21) and (25), one can write

$$\Psi_i^{(\beta)}(x) = (-1)^{|\beta|}H^{T(\beta)}(0)M^{-1}(x)H(x-x_i)\phi_{a_i}(x-x_i) \quad (26)$$

3.1 Illustrative Examples

To demonstrate the efficacy and numerical accuracy of the proposed scheme for derivative reproduction, the test function $f(x) = \sin x$ is first chosen. Third and fourth derivatives of $f(x)$ are obtained via the standard RKPM and the proposed scheme. Plots of absolute errors in these derivatives through the two methods are shown in figures 1(a) and (b). It is amply clear that the absolute error via the present scheme is significantly smaller than that via the regular RKPM. For yet another test function $f(x) = \exp(5x)$, plots of absolute errors in the second and third derivatives, as obtained through the present scheme and the reproducing kernel interpolating (RKI) scheme by Chen et al. (2003), are provided in figures 1(c) and (d). The superior performance of the present scheme is evident in these figures too.

4 A Novel Form of Reproducing Kernel Interpolation:

A new and improved form of reproducing kernel interpolation scheme is developed in this section. First polynomials up to a certain degree are reproduced by a set of weighted B-spline basis functions. Weights are obtained from the reproduction conditions as detailed in section 2. Then a correction vector function is introduced for recovering the interpolation property of the weighted B-spline approximations. A more detailed derivation of the proposed scheme is provided in the following sub-sections.

4.1 Weighted B-spline Basis Functions

A brief introduction to B-spline basis functions, curves and surfaces is provided in Appendix I for a ready reference. However detail descriptions of B-splines may be available in (Piegl, and Tiller 1995). In general B-spline basis functions neither reproduce any polynomials nor do they interpolate the control points. Several techniques for shape modifications are available in the literature (Au and Yuen 1995, Juhász 1999), but they are mostly in the context of NURBS (non-uniform rational B-spline) curves. Moreover, in these approaches, a constant weight is assigned to each control point. Although these techniques are very popular in CAD-CAM applications, the absence of reproducing properties renders them unsuitable for direct adaptations to mesh-free numerical analysis. Presently a weight-based shape modification of B-spline basis functions is considered. Weights are assumed to be spatially varying functions. Accordingly the p^{th} order weighted B-spline basis function may be constructed as:

$$\overline{N}_{i,p}(x) = N_{i,p}(x)w_i(x) \quad (27)$$

where,

$$w_i(x) = H^T(x-x_i)b(x) \quad (28)$$

$$H(x-x_i) = \left\{1, (x-x_i), (x-x_i)^2, \ldots\ldots (x-x_i)^p\right\} \quad (29)$$

$$b(x) = \{b_0(x), b_1(x), \ldots\ldots b_p(x)\} \quad (30)$$

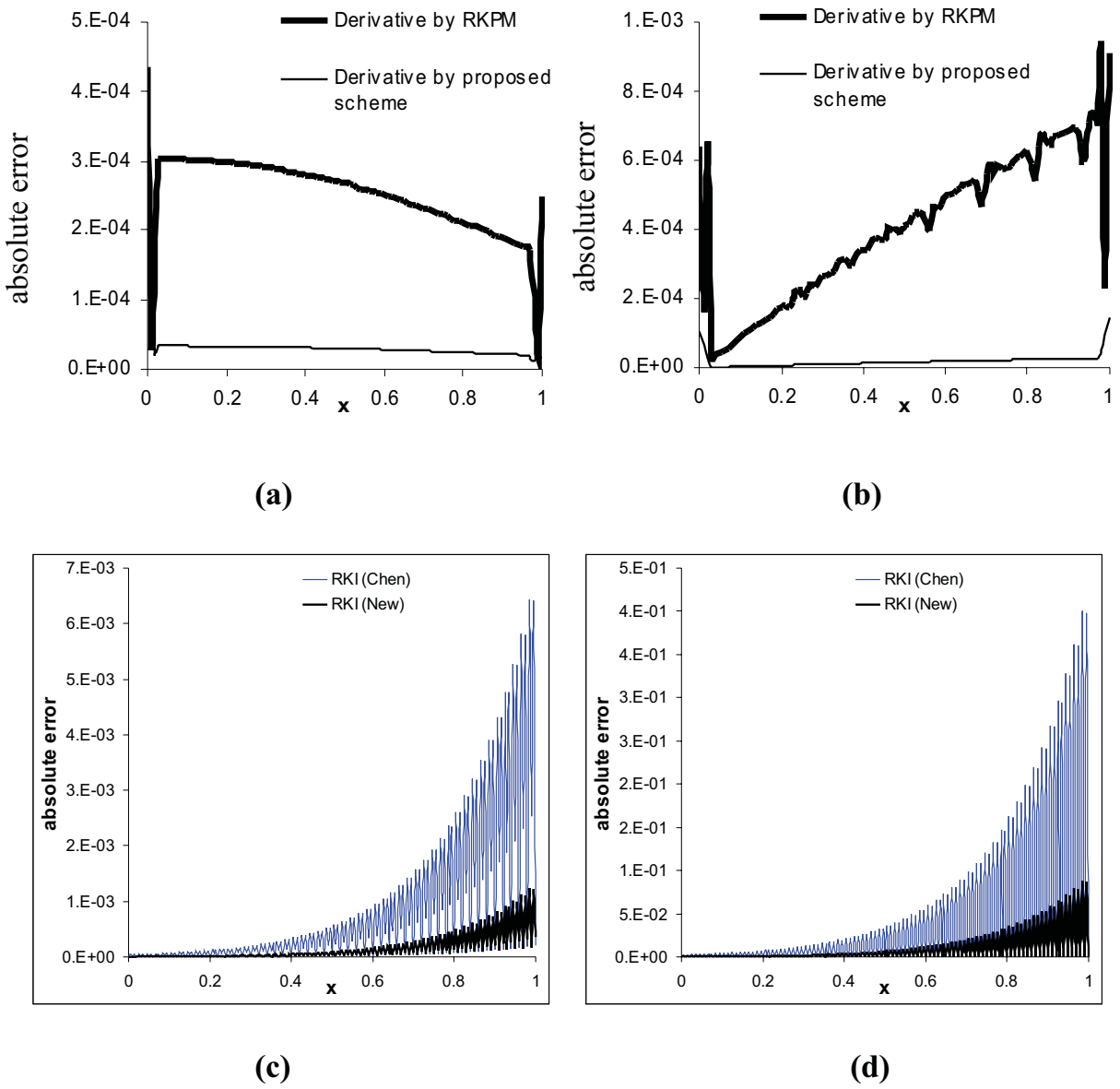

Figure 1: Plots of absolute errors in derivatives (a), (b) third and fourth derivatives via the RKPM (regular) and new derivative reproduction scheme for the target function $f(x) = \sin x$; (c), (d) second and third derivatives via the new RKI and RKI (Chen *et al.*) for the target function $f(x) = e^{5x}$

Coefficient vector $b(x)$ may be determined from the p^{th} order reproducing conditions:

$$\sum_{i=1}^{N_P} \overline{N}_{i,p}(x) x_i^{\alpha} = x^{\alpha}, \quad |\alpha| \le p \tag{31}$$

Equivalently, we may write:

$$\sum_{i=1}^{N_P} N_{i,p}(x) w_i(x) (x - x_i)^{\alpha} = \delta_{|\alpha|,0}, \quad |\alpha| \le p \tag{32}$$

$$\text{i.e., } \sum_{i=1}^{N_P} N_{i,p}(x) w_i(x) H(x - x_i) = H(0) \tag{33}$$

Substituting for $w_i(x)$ from equation (27), we have:

$$\sum_{i=1}^{N_P} N_{i,p}(x) H^T(x - x_i) H(x - x_i) b(x) = H(0) \tag{34}$$

$$\text{where, } b(x) = \overline{M}^{-1}(x) H(0) \tag{35}$$

$$\text{and, } \overline{M}(x) = \sum_{i=1}^{N_P} N_{i,p}(x) H^T(x-x_i) H(x-x_i) \quad (36)$$

Noting equation (27), we finally have:

$$\overline{N}_{i,p}(x) = H^T(0) M^{-1}(x) H(x-x_i) N_{i,p}(x) \quad (37)$$

4.2 The Corrected RK Interpolation Function

Note that the weighted B-spline basis functions, obtained so far, are not interpolating. Towards bringing in the interpolation property, we introduce a vector of correction functions,$\{C_i(x)\}$, and thus modify the RK shape function as:

$$\Psi_i(x) = \frac{1}{\alpha_i(x)+\beta_i(x)} [\alpha_i(x)\overline{N}_{i,p}(x) + \beta_i(x) C_i(x)] \quad (38)$$

The correction function $C_i(x)$ must satisfy the reproducing condition given in equation (9) and it is presently written as:

$$C_i = H(x-x_i) b(x) \phi_{a_i}(x-x_i) \quad (39)$$

The coefficient vector $b(x)$ is obtained, as usual, from the reproducing condition given in equation (9). Any non-negative function with a compact support (barring the p-th order B-spline function $N_{i,p}(x)$) may be taken as the window function $\phi_a(x-x_i)$ to construct $C_i(x)$. Functions $\alpha_i(x)$ and $\beta_i(x)$ in equation (38) are the coefficients introduced to satisfy the interpolation property. Since $\overline{N}_{i,p}(x)$ and $C_i(x)$ both are n reproducing and linearly independent, any linear combination $\overline{N}_{i,p}(x)$ and $C_i(x)$ is also n-reproducing. Using the normalizing condition$\alpha_i(x)+\beta_i(x)=1$, we write equation (38) as:

$$\Psi_i(x) = \alpha_i(x)\overline{N}_{i,p}(x) + (1-\alpha_i(x)) C_i(x) \quad (40)$$

We may make the shape functions interpolating by first evaluating equation (40) at x_j as:

$$\Psi_i(x_j) = \alpha_i(x_j)\overline{N}_{i,p}(x_j) + (1-\alpha_i(x_j)) C_i(x_j) \quad (41)$$

Computations of the coefficients $\alpha_i(x_j)$ from the following equations then impose the interpolating condition:

$$\Psi_i(x_j) = \alpha_i(x_j)\overline{N}_{i,p}(x) + (1-\alpha_i(x_j)) C_i(x_j) = \delta_{ij} \quad (42)$$

$$\text{i.e., } \alpha_i(x_j) = \frac{\delta_{ij} - C_i(x_j)}{\overline{N}_{i,p}(x_j) - C_i(x_j)} \quad (43)$$

Following the evaluation of the discrete values $\alpha_i(x_j)$ at each nodal point, the function $\alpha_i(x)$ may be constructed as:

$$\alpha_i(x) = \sum_{j=1}^{N_P} \Gamma_j(x) \alpha_i(x_j) \quad (44)$$

so that

$$\Psi_i(x_j) = \overline{N}_{i,p}(x) \sum_{j=1}^{N_P} \Gamma_j(x)\alpha_i(x_j) + \left(1 - \sum_{j=1}^{N_P} \Gamma_j(x)\alpha_i(x_j)\right) C_i(x_j) \quad (45)$$

where $\Gamma_j(x)$ is any RKPM basis function or any interpolating function.

4.3 Dilation Parameter for the Weighted B-spline Basis Function

A key strategy of the proposed reproducing kernel interpolation (RKI) method is to take a linear combination of two different families of RK basis functions and determine the coefficients of the linear combination through the interpolating conditions. Towards ensuring that the RKI approximation interpolates the functional values at all grid point, it is essential to have the same support size for both the weighted B-spline basis function $\overline{N}_{i,p}(x)$ and the correction functions$C_i(x)$ for a given i. The support size of the window function ϕ, controlled by dilation parameter a, defines that of an RKPM basis function. Indeed, the dilation parameter a is required to dilate the window function$\phi(x)$ such that it covers at least $\frac{(p+n)!}{p!n!}$ particles, which in turn ensures invertibility of $M(x)$. Since proposition 1 (see section 5) guarantees the non-singularity of $\overline{M}(x)$ (i.e., the moment matrix for weighted B-spline basis function$\overline{N}_{i,p}(x)$), no *dilation parameter* is as such needed to ensure uniqueness of $b(x)$. However for any other window function $\phi(x)$ (possibly used to construct the correction function $C_i(x)$ in equation 39) without the local support property of B-spline functions,

a *dilation parameter* is required to appropriately modify the support size of correction functions. Accordingly, $\overline{N}_{i,p}(x)$ must also be similarly dilated so that its support size becomes identical with that of $C_i(x)$. With $a_i \in R^+$ being the *dilation parameter* associated with i^{th} particle for a one-dimensional kernel function$\phi(x)$, the support radius of$C_i(x)$, constructed using$\phi(x)$, is alsoa_i. On the other hand, support radius of $\overline{N}_{i,p}(x)$ is $\frac{(p+1)}{2}h$, where, h is a characteristic spatial step size. In order to make support sizes of the two component functions equal, the dilation parameter for $\overline{N}_{i,p}(x)$ must be given by $\overline{a}_i = \frac{2a_i}{(p+1)h}$.

Finally, it is useful to note that the modified RK interpolation functions possess the following properties:

1. If $\overline{N}_{i,p}(x) \in C^{k_b}$ and $C_i(x) \in C^{k_c}$ then $\Psi_i(x) \in C^{\min(k_b,k_c)}$

2. From the local support property of B-spline basis functions, $N_{i,p}(x)$will always cover $p+1$ points and thus $\overline{M}(x)$ in equation (36) is always invertible.

3. Shape functions Ψ_i form a partition of unity, i.e.,

$$\sum_{i=1}^{N_P} \Psi_i(x) = 1 \quad \forall x \in \Omega$$

4. Shape functions Ψ_i possess the Kronecker delta property, i.e,

$$\Psi_i(x_j) = \delta_{ij} \quad \forall x_i, x_j \in \Omega$$

4.4 Illustrative Examples

Towards a numerical demonstration of the above method, we adopt B-spline basis functions with $p = 5$ and also a uniform knot (nodal) distribution. In order to construct the correction function$C_i(x)$, the following exponential function is adopted as the kernel function.

$$\phi(x) = \begin{cases} e^{\frac{1}{|x|^2-1}} & \text{if } |x| \leq 1 \\ 0 & \text{otherwise} \end{cases} \tag{46}$$

Two constituent functions $\overline{N}_{i,p}(x)$ and$C_i(x)$, and the modified RK interpolation function $\Psi_i(x)$ (which is the weighted sum of the first two constituent functions) are shown respectively in figures 2(a), (b) and (c). Figures 2(a) and (b) clearly indicate that the maxima and minima of $C_i(x)$ are an order of magnitude less than those of $\overline{N}_{i,p}(x)$. This quite justifies the choice of the kernel function $\phi(x)$ (as in equation (46)) since $C_i(x)$ is just supposed to correct the errors while interpolating a given function $f(x)$ using $\overline{N}_{i,p}(x)$. While other choices for $\phi(x)$ are possible, it is worth noting that $\phi(x)$ must be different from 5^{th} order B-spline functions for the present method to work. As an example on how the interpolation works, we once again choose the same couple of elementary test functions as in figure 1, viz. a periodic function $f(x) = \sin(2\pi x)$ and a monotonically increasing function $f(x) = e^{5x}$ for $x \geq 0$. Figures 3(a, b) show the modified RK interpolant and its two constituent functions $\overline{N}_{i,p}(x)$ and $C_i(x)$ for the two target functions. It is once more observed that values of the correction component are consistently an order less in magnitude than those of the main approximating component through B-splines. Moreover, both the components appear to be consistently sharing the oscillatory or monotonicity characteristics (as the case may be) of the target functions. It is also evident that, for oscillatory target functions (such as the sine function), there is a phase difference of π between the two components.

5 Error Analysis

Let $u(x)$ be a sufficiently smooth function defined on a simply connected open set $\Omega \in R^n$. We denote by $\overline{\Omega}$ the closure of Ω and also by $\partial\Omega$ the boundary of Ω. The boundary of Ω is assumed to be of Lipschitz type. That means that the boundary $\partial\Omega \in R^{n-1}$ is a graph of a Lipschitz function (Brener and Scott, 1994). This is done to avoid boundaries with singularities like the cusp so that Green's formula for integration on the boundary holds. By $C_0^k(\Omega)$, $k > 0$ we mean the set of all k-differentiable functions on Ω which have a compact support in $\overline{\Omega}$. Then for any family of discrete distribution $\left\{\{x_i\}_{i=1}^{N_P}\right\} \subset \overline{\Omega}$, recall that a continuous function $u \in C(\overline{\Omega})$ is presently being approx-

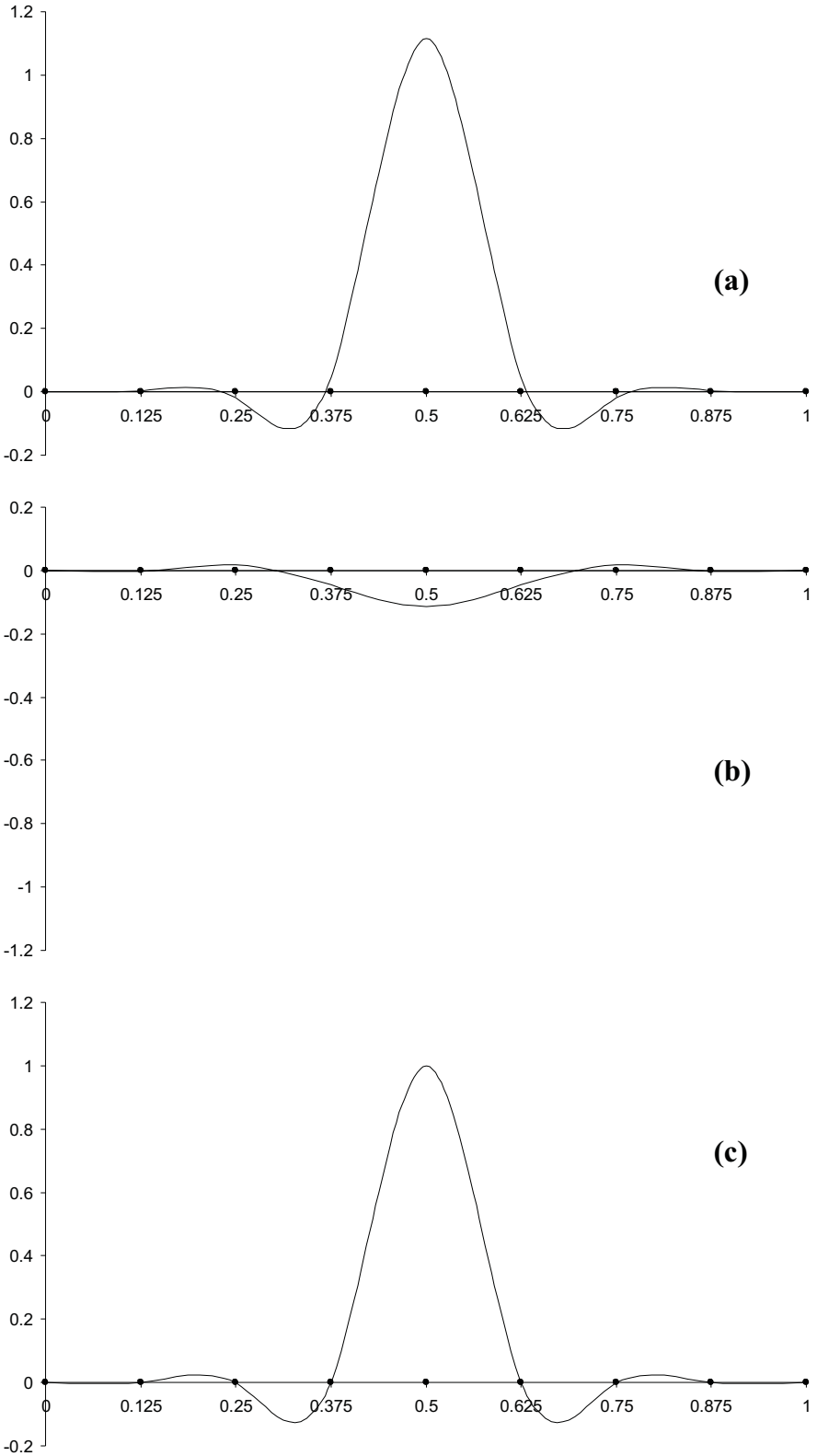

Figure 2: One dimensional example of modified RK interpolation function (a) weighted B-spline basis function; (b) correction functions; (c) modified RK interpolation function

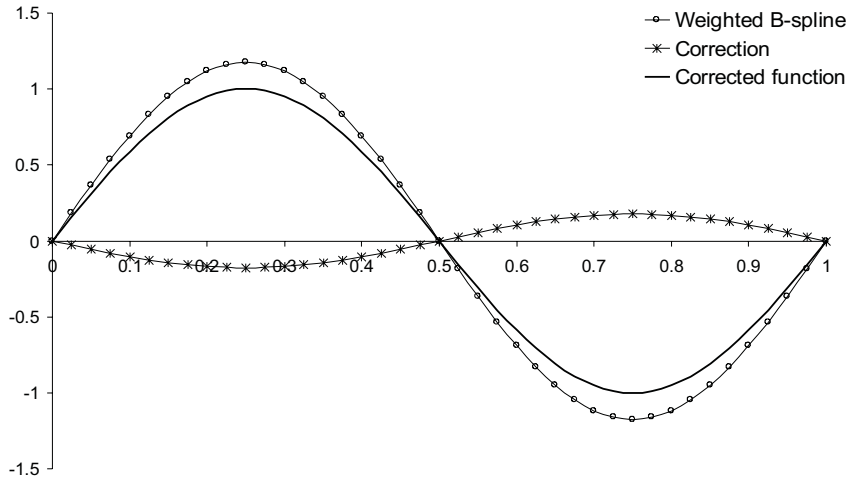

(a)

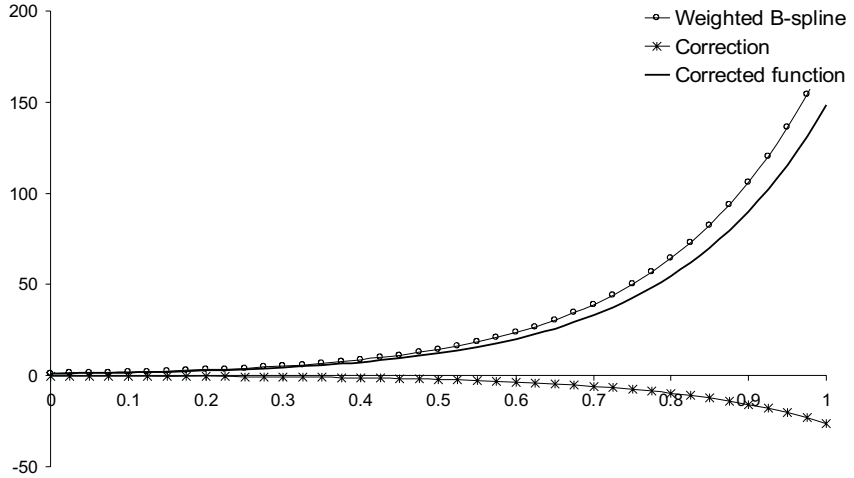

(b)

Figure 3: A demonstration of how the new RK interpolation works with target functions: (a) $f(x) = \sin(2\pi x)$ and (b) $f(x) = e^{5x}$

imated as:

$$u^a(x) = \sum_{i=1}^{N_P} \Psi_i(x) u_i \tag{47}$$

where $\Psi_i(x)$ is the interpolating form of RK shape function given by:

$$\Psi_i(x) = \alpha(x_i)\overline{N}_{i,p}(x) + (1 - \alpha(x_i))C_i(x) \tag{48}$$

Also recall that $\overline{N}_{i,p}(x)$ and $C_i(x)$ are two different families of RKPM basis functions and separately satisfy the reproducing conditions as:

$$\sum_{i=1}^{N_p} \overline{N}_{i,p}(x) x_i^\alpha = x^\alpha \tag{49a}$$

$$\sum_{i=1}^{N_p} C_i(x) x_i^\alpha = x^\alpha \tag{49b}$$

Now consider a particle distribution $\left\{ \{x_i\}_{i=1}^{N_P} \right\}$ in the closed domain $\overline{\Omega} = \Omega \cup \partial\Omega$ and denote $\Gamma_D \subset \partial\Omega$ as the part of the boundary ($\partial\Omega$) with only

Dirichlet boundary conditions prescribed. The interpolating RK shape functions are given by equation (48). Then for any particle (node) $x_j \in \overline{\Omega}$ the Kronecker delta property holds:

$$\Psi_i(x_j) = \delta_{ij}, \quad 1 \le i \le N_P \tag{50}$$

Errors are presently estimated for the case of quasi-uniform support sizes, i.e., $\exists$ two constants $c_1, c_2 \in (0,\infty)$ such that,

$$c_1 \le \frac{a_i}{a_j} \le c_2 \quad \forall i, j \tag{51}$$

where, a_i is dilation parameter associated with the i^{th} node. Then for such a particle distribution $\exists$ a typical (characteristic) support size $a$such that [Han and Meng 2001],

$$\tilde{c}_1 \le \frac{a_i}{a} \le \tilde{c}_2 \quad \forall i \text{ and } 0 < \tilde{c}_1 \le \tilde{c}_2 < \infty \tag{52}$$

To start deriving the error estimates, some definitions would prove useful.

Definition 1: A point $x \in \overline{\Omega}$ is said to be covered by m shape functions if there are m indices $i_1, \ldots\ldots, i_m$ such that

$$\left|x - x_{i_j}\right| < a_{i_j}, \quad j = 1, \ldots\ldots, m \tag{53}$$

Definition 2: For any $x \in \overline{\Omega}$, a necessary condition for $M(x)$ to be invertible is that x is covered by at least $N_P = \dim P_p = \frac{(p+n)!}{p!n!}$ shape functions, where p is the highest degree among the set of monomials that can be reproduced by mesh-free shape functions and n is the spatial dimension.

Proposition 1. The moment matrix $\overline{M}(x)$ corresponding to an $\overline{a}$-dilated B-spline basis functions is invertible for all $p \ge 1$ and $\overline{a} > 0$.

Proof. Higher dimensional B-spline basis function may be constructed by taking the tensor product of B-spline basis functions in one dimension as given in the Appendix I. Because of its local support property, one dimensional B-spline basis function $N_{i,p}(x)$ is exactly covered by $p+1$ points and its n-dimensional counterpart is exactly covered by $(p+1)^n$ points. Now the necessary condition for $\overline{M}(x)$ to be invertible is that $\boldsymbol{x}$ is covered by at least $\frac{(p+n)!}{p!n!}$ shape functions. Since, one has

$$\frac{(p+n)!}{p!n!} = \prod_{j=1}^{n} \frac{(p+j)}{j} < (p+1)^n, \quad \forall n > 1$$

$$\text{and } \frac{(p+1)!}{p!} = (p+1), \quad n = 1, \tag{54}$$

the proposition follows. □

Definition 3: The particle distribution $\left\{\{x_i\}_{i=1}^{N_P}\right\}$ is said to be (a,p)regular if $\exists$ a constant $L(c_0, \sigma_0)$ and integers $i_0, ..., i_p \in [1, N_P]$ such that $\max_{x \in \overline{\Omega}} \left|\left|M_0(x)^{-1}\right|\right|_2 \le L(c_0, \sigma_0)$, where c_0 and σ_0 are two positive real constants satisfying the following conditions for any $x \in \overline{\Omega}$:

$$\min_{0 \le j \le p} \phi\left(\frac{x - x_{i_j}}{a \quad i_j}\right) \ge c_0 > 0 \tag{55a}$$

$$\min_{0 \le j \le p} \frac{\left|x - x_{i_j}\right|}{a_{i_j}} \ge \sigma_0 > 0 \tag{55b}$$

Moreover,

$$M_0(x) = \sum_{i=1}^{N_P} \phi\left(\frac{x - x_{i_j}}{a_i}\right) H\left(\frac{x - x_{i_j}}{a}\right) H\left(\frac{x - x_{i_j}}{a}\right)^T \tag{56}$$

denotes the scaled moment matrix.

In particular, for multi-linear shape functions, a particle distribution $\left\{\{x_i\}_{i=1}^{N_P}\right\}$ is $(a,1)$ regular if $\exists$ two constants $c_0, \tilde{c}_0 > 0$ such that for any $x \in \overline{\Omega}$, there are $n+1$ particles $x_{i_0}, \ldots, x_{i_n}$ satisfying

$$\min_{0 \le j \le n} \phi\left(\frac{x - x_{i_j}}{a}\right) \ge c_0 > 0 \tag{57}$$

and the n-simplex with the vertices $x_{i_0}, \ldots, x_{i_n}$ has a volume larger than $\tilde{c}_0 a^n$. A more relevant point to note in the present context is that if $\phi(x)$ is a p-th order B-spline, then $\left\{\{x_i\}_{i=1}^{N_P}\right\}$ is (a,p) regular.

Definition 4: Given an (a,p) regular particle distribution, $\tilde{b}(x) = \{b_0(x), ab_1(x), \ldots\ldots, a^p b_p(x)\}^T$ is the unique solution of the system

$$M_0(x)\tilde{b}(x) = H(0) \tag{58}$$

and $\exists$ a constant $c < \infty$ such that

$$\max_{\alpha : |\alpha| \le p} a^{|\alpha|} \left|\left|b_\alpha\right|\right|_{L^\infty(\Omega)} \le c \tag{59}$$

5.1 Bounds on the shape functions

Now the polynomial reproducing condition based on new RKI shape function may be written as:

$$\sum_{i=1}^{N_P} \Psi_i(x) x_i^{\alpha} = x^{\alpha}, \quad \forall \alpha : |\alpha| \leq p \tag{60}$$

$$\Psi_i(x) = \alpha_i(x)\overline{N}_{i,p}(x) + (1-\alpha_i(x))C_i(x) \tag{61}$$

where, $\overline{N}_{i,p}(x)$ and $C_i(x)$ are two different families of RKPM basis functions and $\alpha_i(x)$ is the coefficient function and may be obtained as:

$$\alpha_i(x) = \sum_{j=1}^{N_P} \Gamma_j(x)\alpha_i(x_j) \tag{62}$$

where $\Gamma_j(x)$ is any RKPM basis function or any interpolating functions. Coefficient $\alpha_i(x_j)$ may be obtained satisfying the interpolating condition as (see section 4.2):

$$\alpha_i(x_j) = \frac{\delta_{ij} - C_i(x_j)}{\overline{N}_{i,p}(x_j) - C_i(x_j)} \tag{63}$$

Before we bound the shape functions, we have following remarks:

Proposition 2: For a particle distribution $\left\{\{x_i\}_{i=1}^{N_P}\right\}$ and the choice of $\phi(x)$ and $N_{i,p}(x)$ as in equations (46) and (A-2) respectively, one has:
$\overline{N}_{i,p}(x_j) \neq C_i(x_j) \quad \forall j$ such that $x_j \in supp(\Psi_i)$

Proof.

$$\text{Let } \overline{N}_{i,p}(x_j) = C_i(x_j) \tag{64}$$

$$\Rightarrow \overline{N}_{i,p}(x_j) - C_i(x_j) = 0 \tag{65}$$

Using equations (11) and (37), equation (65) may be written as:

$$H^T(0)M^{-1}(x)H(x_j - x_i)N_{i,p}(x_j) - H^T(0)M^{-1}(x_j)H(x_j - x_i)\phi_a(x_j - x_i) = 0 \tag{66}$$

$$\Rightarrow H^T(0)\left[M^{-1}(x)N_{i,p}(x_j) - M^{-1}(x_j)\phi_a(x_j - x_i)\right]H(x_j - x_i) = 0 \tag{67}$$

$$\Rightarrow M(x_j)N_{i,p}(x_j) = \overline{M}(x_j)\phi_a(x_j - x_i) \tag{68}$$

Pre-multiplying by $H^T(0)$ and post-multiplying by $H(0)$, equation (68) may be written as:

$$H^T(0)M(x_j)H(0)N_{i,p}(x_j) = H^T(0)\overline{M}(x_j)H(0)\phi_a(x_j - x_i) \tag{69}$$

Components of moment matrices $M(x_j)$ and $\overline{M}(x_j)$ are thus given by:

$$M_{\alpha\beta}(x_j) = \sum_{k=1}^{N_P} (x_j - x_k)^{\alpha-1}(x_j - x_k)^{\beta-1}\phi_a(x_j - x_k) \tag{70}$$

$$M_{\alpha\beta}(x_j) = \sum_{k=1}^{N_P} (x_j - x_k)^{\alpha-1}(x_j - x_k)^{\beta-1}N_{k,p}(x_j) \tag{71}$$

Substituting equations (70) and (71) in (69) we have,

$$M_{11}(x_j)N_{i,p}(x_j) = \overline{M}_{11}(x_j)\phi_a(x_j - x_i) \tag{72}$$

$$N_{i,p}(x_j)\sum_{k=1}^{N_P}\phi_a(x_j - x_k) = \phi_a(x_j - x_i)\sum_{k=1}^{N_P}N_{k,p}(x_j) \tag{73}$$

$\Rightarrow N_{i,p}(x_j) = \phi_a(x_j - x_i)$ [$\phi_a(x)$ and $N_{i,p}(x)$ constitute a partition of unity]

Since $N_{i,p}(x)$ and $\phi_a(x - x_i)$ are presently two different functions (given respectively by equations A-2 and 46) with different values almost everywhere except at set of points of measure zero. In particular, at all the grid points x_j covered by $\Psi_i(x)$, one has:

$$N_{i,p}(x_j) \neq \phi_a(x_j - x_i) \tag{74}$$

This implies

$$\overline{N}_{i,p}(x_j) - C_i(x_j) \neq 0 \tag{75}$$

Hence the proposition follows. □

Now assuming the (a,p) regularity of particle distribution, we have the following results:

Proposition 3: For an (a,p) regular particle distribution, coefficient function $\alpha_i(x)$ given by equation (62) is uniformly bounded, i.e, $\exists$ a constant $\overline{c} < \infty$ such that,

$$||\alpha_i(x)||_{L^{\infty}(\Omega)} \leq \overline{c} \tag{76}$$

Proof. From equation (62), one has:

$$||\alpha_i(x)||_{L^\infty(\Omega)} = \left|\left|\sum_{j=1}^{N_P} \Gamma_j(x)\alpha_i(x_j)\right|\right|_{L^\infty(\Omega)} \tag{77}$$

$$\Rightarrow ||\alpha_i(x)||_{L^\infty(\Omega)} = \left|\left|\sum_{j=1}^{N_P} \frac{\delta_{ij}-C_i(x_j)}{\overline{N}_{i,p}(x_j)-C_i(x_j)}\Gamma_j(x)\right|\right|_{L^\infty(\Omega)} \tag{78}$$

$$\Rightarrow ||\alpha_i(x)||_{L^\infty(\Omega)} \leq \sum_{j=1}^{N_P} \left|\left|\frac{\delta_{ij}-C_i(x_j)}{\overline{N}_{i,p}(x_j)-C_i(x_j)}\Gamma_j(x)\right|\right|_{L^\infty(\Omega)} \tag{79}$$

$$\Rightarrow ||\alpha_i(x)||_{L^\infty(\Omega)} \leq \sum_{j=1}^{N_P} \left|\left|\frac{\delta_{ij}-C_i(x_j)}{\overline{N}_{i,p}(x_j)-C_i(x_j)}\right|\right|_{L^\infty(\Omega)} \left|\left|\Gamma_j(x)\right|\right|_{L^\infty(\Omega)} \tag{80}$$

$$\Rightarrow ||\alpha_i(x)||_{L^\infty(\Omega)} \leq \sum_{j=1}^{N_P} \left|\left|\delta_{ij}-C_i(x_j)\right|\right|_{L^\infty(\Omega)} \cdot \left|\left|\frac{1}{\overline{N}_{i,p}(x_j)-C_i(x_j)}\right|\right|_{L^\infty(\Omega)} \left|\left|\Gamma_j(x)\right|\right|_{L^\infty(\Omega)} \tag{81}$$

Since $\overline{N}_{i,p}(x_j) - C_i(x_j)$ is uniformly bounded away from zero, so is $\left|\left|\frac{1}{\overline{N}_{i,p}(x_j)-C_i(x_j)}\right|\right|_{L^\infty(\Omega)}$. Moreover from [Han and Meng 2001, Theorem 4.6], one may readily show that RKPM basis functions $\max_{1\leq j\leq N_P} \left|\left|\Gamma_j(x)\right|\right| \leq \hat{c}$ for some constant $\hat{c} < \infty$.

Hence one may write

$$||\alpha_i(x)||_{L^\infty(\Omega)} \leq \overline{c} \text{ for some constant } \overline{c} < \infty \tag{82}$$

Hence the proposition follows. □

In the new RKI approximation as in equation (61), $\overline{N}_{i,p}(x)$ and $C_i(x)$ separately satisfy the polynomial reproducing conditions as:

$$\sum_{i=1}^{N_P} \alpha_i(x)\overline{N}_{i,p}(x)x_i^\alpha = \alpha(x)x^\alpha \tag{83a}$$

$$\text{and } \sum_{i=1}^{N_P} (1-\alpha_i(x))C_i(x)x_i^\alpha = (1-\alpha(x))x^\alpha \tag{83b}$$

Equation (83) may be written as:

$$\sum_{i=1}^{N_P} \alpha_i(x)\overline{N}_{i,p}(x)H(x-x_i) = \alpha(x)H(0) \tag{84a}$$

$$\text{and } \sum_{i=1}^{N_P} (1-\alpha_i(x))C_i(x)H(x-x_i)^\alpha = (1-\alpha(x))H(0) \tag{84b}$$

Equivalently one has

$$\left[\sum_{i=1}^{N_P} \alpha_i(x)N_{i,p}(x-x_i)H^T(x-x_i)H(x-x_i)\right] b(x) = \alpha(x)H(0) \tag{85a}$$

and

$$\left[\sum_{i=1}^{N_P} (1-\alpha_i(x))\phi_{a_i}(x-x_i)H^T(x-x_i)H(x-x_i)\right] \cdot b_1(x) = (1-\alpha(x))H(0) \tag{85b}$$

Denote scaled moment matrices corresponding to $\overline{N}_{i,p}(x)$ and $C_i(x)$ respectively as:

$$\overline{M}_0(x) = \sum_{i=1}^{N_P} \alpha_i(x)H\left(\frac{x-x_i}{a}\right)H\left(\frac{x-x_i}{a}\right)^T \cdot N_{i,p}\left(\frac{x-x_i}{a_i}\right) \tag{86a}$$

$$M_{C0}(x) = \sum_{i=1}^{N_P} (1-\alpha_i(x))H\left(\frac{x-x_i}{a}\right)H\left(\frac{x-x_i}{a}\right)^T \cdot \phi_{a_i}(x-x_i) \tag{86b}$$

and $\tilde{b}(x) = \left(a^{|\alpha|}\overline{b}_\alpha(x)\right)_{|\alpha|\leq p}$ and $\tilde{b}_c(x) = \left(a^{|\alpha|}b_c\alpha(x)\right)_{|\alpha|\leq p}$. Then polynomial reproducing conditions imply:

$$\overline{M}_0(x)\tilde{b}(x) = \alpha(x)H(0) \Rightarrow \overline{b}(x) = \alpha(x)\overline{M}_0(x)^{-1}H(0) \tag{87a}$$

$$M_{C0}(x)\tilde{b}_c(x) = (1-\alpha(x))H(0) \Rightarrow \tilde{b}_c(x) = (1-\alpha(x))M_{C0}(x)^{-1}H(0) \tag{87b}$$

From definition (4)

$$\max_{\alpha:|\alpha|\le p}\left|\left|\tilde{b}\right|\right|_{L^\infty(\Omega)}=\max_{\alpha:|\alpha|\le p}a^{|\alpha|}\left|\left|\overline{b}_\alpha\right|\right|_{L^\infty(\Omega)}\le\overline{c},\quad \overline{c}<\infty \tag{88a}$$

$$\max_{\alpha:|\alpha|\le p}\left|\left|\tilde{b}_c\right|\right|_{L^\infty(\Omega)}=\max_{\alpha:|\alpha|\le p}a^{|\alpha|}\left|\left|b_{c\alpha}\right|\right|_{L^\infty(\Omega)}\le c,\quad c<\infty \tag{88b}$$

for some constants $\overline{c}$, c. Rewrite equation (61) as:

$$\Psi_i(x)=\alpha_i(x)H\left(\frac{x-x_i}{a}\right)^T\overline{b}(x)N_{i,p}(x)+(1-\alpha_i(x))H\left(\frac{x-x_i}{a}\right)^T b_c(x)\phi_a(x-x_i)$$

$$\begin{aligned}&\max_{1\le i\le N_P}\left|\left|\Psi_i\right|\right|_{L^\infty(\Omega)}\\&=\max_{1\le i\le N_P}\left|\left|\alpha_i(x)H\left(\frac{x-x_i}{a}\right)^T\overline{b}(x)N_{i,p}(x)\right.\right.\\&\left.\left.+\ (1-\alpha_i(x))H\left(\frac{x-x_i}{a}\right)^T b_c(x)\phi_a(x-x_i)\right|\right|_{L^\infty(\Omega)}\\&\le\max_{1\le i\le N_P}\left|\left|\alpha_i(x)H\left(\frac{x-x_i}{a}\right)^T\overline{b}(x)N_{i,p}(x)\right|\right|_{L^\infty(\Omega)}\\&+\max_{1\le i\le N_P}\left|\left|(1-\alpha_i(x))H\left(\frac{x-x_i}{a}\right)^T b_c(x)\cdot\phi_a(x-x_i)\right|\right|_{L^\infty(\Omega)}\end{aligned}$$

From equation (82), (88a) and (88b) one can readily write,

$$\max_{1\le i\le N_P}\left|\left|\Psi_i\right|\right|_{L^\infty(\Omega)}\le c \text{ for some } c<\infty \tag{89}$$

Hence the new RKI shape functions are uniformly bounded.

5.2 Bounds on derivatives of RKPM shape functions

Consider equation (18) describing the novel scheme for derivative reproduction:

$$\sum_{i=1}^{N_P}\Psi_i^{(\beta)}(x)H(x-x_i)=(-1)^{|\beta|}H^{(\beta)}(0),\quad\forall|\beta|\le k \tag{90}$$

where $\Psi_i^{(\beta)}(x)$ is the β^{th} derivative of RKPM shape function $\Psi_i(x)$ and is given by

$$\Psi_i^{(\beta)}(x)=H^T(x-x_i)b^\beta(x)\phi_{a_i}(x-x_i) \tag{91}$$

where $b^\beta(x)$ is vector of unknown coefficients and may be obtained from the equation

$$M(x)b^\beta(x)=(-1)^{|\beta|}H^{(\beta)}(0) \tag{92}$$

and

$$M(x)=\sum_{i=1}^{N_P}H(x-x_i)H^T(x-x_i)\phi_{a_i}(x-x_i) \tag{93}$$

Now $\tilde{b}^\beta(x)=\left\{a^{|\alpha|+|\beta|}b_\alpha^\beta(x)\right\}$ is the solution of the system

$$M_0(x)\tilde{b}^\beta(x)=(-1)^{|\beta|}H^{(\beta)}(0) \tag{94}$$

and $\Psi_i^{(\beta)}(x)$ is given by

$$\begin{aligned}\Psi_i^{(\beta)}(x)&=\phi\left(\frac{x-x_i}{a_i}\right)\sum_{|\alpha|\le p}\left(\frac{x-x_i}{a}\right)^\alpha\tilde{b}_\alpha^\beta\\&=a^{|\beta|}\phi\left(\frac{x-x_i}{a_i}\right)\sum_{|\alpha|\le p}\left(\frac{x-x_i}{a}\right)^\alpha a^{|\alpha|}b_\alpha^\beta\end{aligned} \tag{95}$$

As before $M_0(x)$ is the scaled moment matrix given by equation (56). Now from equation (95), one has the unique and bounded solution:

$$\tilde{b}^\beta(x)=(-1)^{|\beta|}M_0(x)^{-1}H^{(\beta)}(0) \tag{96}$$

According to definition (4) for an (a,p)regular particle distribution, one may write,

$$\max_{x\in\Omega}\left|\left|M_0(x)^{-1}\right|\right|_2\le L(c_0,\sigma_0) \tag{97}$$

$$\Rightarrow\max_{|\alpha|\le p}\left|\left|\tilde{b}_\alpha^\beta\right|\right|_{L^\infty(\Omega)}=\max_{|\alpha|\le p}a^{|\alpha|+|\beta|}\left|\left|b_\alpha^\beta\right|\right|_{L^\infty(\Omega)}\le c \tag{98}$$

$$\Rightarrow\max_{|\alpha|\le p}a^{|\alpha|}\left|\left|b_\alpha^\beta\right|\right|_{L^\infty(\Omega)}\le\frac{c}{a^{|\beta|}} \tag{99}$$

Then from equation (99) we immediately obtain the following result.

Theorem 1:
If particle distribution is(a,p)regular and$\phi\in C^k(\Omega)$ then $\exists$ a constant $c<\infty$ such that

$$\max_{1\le i\le N_P}\max_{|\beta|\le k}\left|\left|\Psi_i^{(\beta)}\right|\right|_{L^\infty(\Omega)}\le\frac{c}{a^{|\beta|}} \tag{100}$$

5.3 Bounds on the derivatives of new RKI shape functions

For any multi-index β with $|\beta| = 1$, differentiating equation (61) we have:

$$D^{\beta}\Psi_i(x) = \alpha_i(x)\overline{N}_{i,p}^{(\beta)}(x) + \alpha_i^{(\beta)}(x)\overline{N}_{i,p}(x) + \{1-\alpha_i(x)\}C_i^{(\beta)}(x) - \alpha_i^{(\beta)}(x)C_i(x)$$

$$\Rightarrow D^{\beta}\Psi_i(x) = \alpha_i(x)\overline{N}_{i,p}^{(\beta)}(x) + \left\{\overline{N}_{i,p}(x) - C_i(x)\right\} \cdot \sum_{j=1}^{N_P}\Gamma_j^{(\beta)}(x)\alpha_i(x_j) + \{1-\alpha_i(x)\}C_i^{(\beta)}(x)$$

Taking the norm:

$$\max_{1\le i\le N_P}\max_{|\beta|\le k}\left|\left|D^{\beta}\Psi_i(x)\right|\right|_{L^{\infty}(\Omega)} = \left|\left|\alpha_i(x)\overline{N}_{i,p}^{(\beta)}(x) + \left\{\overline{N}_{i,p}(x) - C_i(x)\right\}\sum_{j=1}^{N_P}\Gamma_j^{(\beta)}(x)\alpha_i(x_j) + \{1-\alpha_i(x)\}C_i^{(\beta)}(x)\right|\right|_{L^{\infty}(\Omega}$$

$\Rightarrow$

$$\begin{aligned}&\max_{1\le i\le N_P}\max_{|\beta|\le k}\left|\left|D^{\beta}\Psi_i(x)\right|\right|_{L^{\infty}(\Omega)}\\ &\le ||\alpha_i(x)||_{L^{\infty}(\Omega)}\left|\left|\overline{N}_{i,p}^{(\beta)}(x)\right|\right|_{L^{\infty}(\Omega)}\\ &+\left|\left|\{\overline{N}_{i,p}(x) - C_i(x)\}\right|\right|_{L^{\infty}(\Omega)} \cdot \left|\left|\sum_{j=1}^{N_p}\Gamma_j^{(\beta)}(x)\alpha_i(x_j)\right|\right|_{L^{\infty}(\Omega)}\\ &+\left|\left|C_i^{(\beta)}(x)\right|\right|_{L^{\infty}(\Omega)} - ||\alpha_i(x)||_{L^{\infty}(\Omega)}\left|\left|C_i^{(\beta)}(x)\right|\right|_{L^{\infty}(\Omega)}\end{aligned}$$

Then from proposition 3 and theorem 1 one may readily write:

$$\max_{1\le i\le N_P}\max_{|\beta|\le k}||D^{\beta}\Psi_i(x)||_{L^{\infty}(\Omega)} \le \frac{c}{a^{\beta}}, \quad \forall|\beta| \le k \tag{101}$$

for some $c < \infty$

Hence derivatives of new RKI basis functions are uniformly bounded.

5.4 Error estimate for mesh free approximations:

To begin with some relevant definitions are given below [see Brenner and Scott, 1994].

Definition 5: A domain Ω is said to be star shaped with respect to a ball B if, for all $x \in \Omega$ the closed convex hull of $\{x\} \cup B$ is a subset ofΩ.

Definition 6: Chunkiness parameter of Ω is defined by $\gamma = \frac{d}{\rho_{\max}}$, where d is the diameter of Ω and $\rho_{\max} = \sup\{\rho :$ Ω is star-shaped with respect to a ball of radius $\rho\}$.

Let $u \in W^{m+1,q}(\Omega)$, $m \ge 0$, $q \in [1,\infty]$ and $m+1 > \frac{n}{q}$ if $q > 1$, or $m+1 \ge n$ if $q = 1$. Then by Sobolev embedding theorem, $u \in C(\overline{\Omega})$ and pointwise values of $u(x)$ may be used. Now approximation of $u(x)$ at any point x^* based on new RKI scheme may be written as:

$$u^a(x^*) = \sum_{i=1}^{N_P}\Psi_i(x^*)u(x^*) \tag{102}$$

In this section we will estimate error $u(x^*) - u^a(x^*)$ in Sobolev norms. Let $p_1 = \min\{p+1, m+1\}$. Now assume the particle distribution is (a,p) regular with $\phi \in C^k$. Let $B_{x^*} = \left\{x : |x^* - x| < \max_{1\le i\le N_P} a_i\right\}$ be an open ball about x^*. We first bound the error $u(x^*) - u^a(x^*)$ ion Sobolev norms over $B* \cap \overline{\Omega}$. Define

$$\overline{\Omega}_{x^*} = \left\{x : |x^* - x| < \max_{1\le i\le N_P} 2a_i\right\} \tag{103}$$

and let

$$S_{x^*} = \{i : dist\,(x^*, B_{x^*}) < a_i\} \tag{104}$$

Now since, $\exists$ a constant I_0 such that for any $x \in \overline{\Omega}$ there are at most I_0 of x_i satisfying the relation $||x - x_i|| < a_i$, i.e., each point in $\overline{\Omega}$ is covered by at most I_0 shape function, $card(S_{x^*})$ is uniformly bounded. If $\overline{\Omega}_{x^*} \subset \overline{\Omega}$, then $\overline{\Omega}_{x^*} \cap \overline{\Omega} = \overline{\Omega}_{x^*}$ is star-shaped with respect to $B_{x^*} \triangleq \tilde{B}_{x^*}$, and the chunkiness parameter of $\overline{\Omega}_{x^*} \cap \overline{\Omega}$ is uniformly bounded. At the boundary, where $\overline{\Omega}_{x^*} \not\subset \overline{\Omega}$, we can chose a ball $\tilde{B}_{x^*}$ of radius $\max_{1\le i\le N_P} a_i/2$ with x^* at the boundary such that $\overline{\Omega}_{x^*} \cap \overline{\Omega}$ is star-shaped with respect

to $\tilde{B}_{x^*}$. Again chunkiness parameter of $\overline{\Omega}_{x^*} \cap \overline{\Omega}$ is uniformly bounded with respect to $\tilde{B}_{x^*}$.

Now denote the p_1^{th} order remainder term as,

$$R^{p_1}u(x^*) = u(x^*) - Q^{p_1}u(x^*) \tag{105}$$

where, $Q^{p_1}u(x^*)$ is the Taylor polynomial of degree $p_1 - 1$ of u averaged over $\tilde{B}_{x^*}$. Then the chunkiness parameter is uniformly bounded when the characteristic support size a is sufficiently small. Under these conditions one may write the following inequality using the Bramble-Hilbert lemma [see Brenner and Scott, 1994],

$$\begin{aligned} &||R^{p_1}u(x^*)||_{W^{l,q}(\Omega_{x^*}\cap\Omega)} \\ &\quad \leq c_{p_1,l,\gamma}a^{p_1-l}|u|_{W^{p_1,q}(\Omega_{x^*}\cap\Omega)}, \quad l = 0,\ldots,p_1 \end{aligned} \tag{106}$$

$$\begin{aligned} &||R^{p_1}u(x^*)||_{L^{\infty}(\Omega_{x^*}\cap\Omega)} \\ &\quad \leq c_{p_1,n,\gamma,q}a^{p_1-n/q}|u|_{W^{p_1,q}(\Omega_{x^*}\cap\Omega)} \end{aligned} \tag{107}$$

Now for $x^* \in \tilde{B}_{x^*} \cap \overline{\Omega}$ one may write

$$\begin{aligned} u(x^*) - u^a(x^*) &= Q^{p_1}u(x^*) - \sum_{i=1}^{N_P} Q^{p_1}u(x_i)\Psi_i(x) \\ &\quad + R^{p_1}u(x^*) - \sum_{i=1}^{N_P} R^{p_1}u(x_i)\Psi_i(x) \end{aligned} \tag{108}$$

By the polynomial reproduction property, one may write,

$$\sum_{i=1}^{N_P} Q^{p_1}u(x_i)\Psi_i(x) = Q^{p_1}u(x^*) \tag{109}$$

Thus equation (108) becomes,

$$u(x^*) - u^a(x^*) = R^{p_1}u(x^*) - \sum_{i=1}^{N_P} R^{p_1}u(x_i)\Psi_i(x^*) \tag{110}$$

Since $x_i \in \Omega_{x^*} \cap \overline{\Omega}$ for $i \in S_{x^*}$,

$$\begin{aligned} &||u(x^*) - u^a(x^*)||_{W^{l,q}(\Omega_{x^*}\cap\Omega)} \\ &\leq ||R^{p_1}u(x^*)||_{W^{l,q}(\Omega_{x^*}\cap\Omega)} \\ &\quad + ||R^{p_1}u(x^*)||_{L^{\infty}(\Omega_{x^*}\cap\Omega)} \sum_{i\in S_{x^*}} ||\Psi_i||_{W^{l,q}(\Omega_{x^*}\cap\Omega)} \end{aligned}$$

Since card (S_{x^*}) is uniformly bounded, from equation (102), (105) and (106), one may write,

$$\begin{aligned} &||u(x^*) - u^a(x^*)||_{W^{l,q}(\Omega_{x^*}\cap\Omega)} \\ &\leq c_{p_1,l,\gamma}a^{p_1-l}|u|_{W^{p_1,q}(\Omega_{x^*}\cap\Omega)}, \\ &\qquad 0 \leq l \leq \min(p_1,k) \quad \forall x^* \in \overline{\Omega} \end{aligned} \tag{111}$$

Equivalently,

$$\begin{aligned} &||u(x^*) - u^a(x^*)||_{W^{l,q}(\Omega)} \\ &\leq c_{p_1,l,\gamma}a^{p_1-l}|u|_{W^{p_1,q}(\Omega_{x^*}\cap\Omega)}, \\ &\qquad 0 \leq l \leq \min(p_1,k) \quad \forall x^* \in \overline{\Omega} \end{aligned} \tag{112}$$

Convergence study:

In this section, a limited numerical study on the convergence of the new interpolating RK method is undertaken. Such a study helps demonstrate the theoretical error estimate given in previous section. For all numerical work, uniform particle distribution with uniform support size has been taken. As support size is proportional to spatial step size h (i.e., the characteristic distance between the closest grid points), for $u \in H^{p+1}(\Omega)$, error estimate for mesh free interpolants may be recast as:

$$||u - u^a||_{H^1(\Omega)} \leq ch^p|u|_{H^{p+1}(\Omega)} \tag{113}$$

$$||u - u^a||_{L^2(\Omega)} \leq ch^{p+1}|u|_{H^{p+1}(\Omega)} \tag{114}$$

For a one dimensional elliptic boundary value problem, optimal order mesh-free error estimate of mesh-free solution u^a may be expressed as:

$$\left|\left|u - u^R\right|\right|_{H^1(\Omega)} \leq ch^p|u|_{H^{p+1}(\Omega)} \tag{115}$$

Optimal order mesh-free error estimate in L^2norm may also be expressed by Nitsche's technique (Brenner and Scott 1994) as:

$$\left|\left|u - u^R\right|\right|_{L^2(\Omega)} \leq ch^{p+1}|u|_{H^{p+1}(\Omega)} \tag{116}$$

The order of convergence is verified via two examples. For the first example following one-dimensional boundary value problem is considered:

$$u_{,xx} = e^x, \quad x \in [0,1] \tag{117}$$

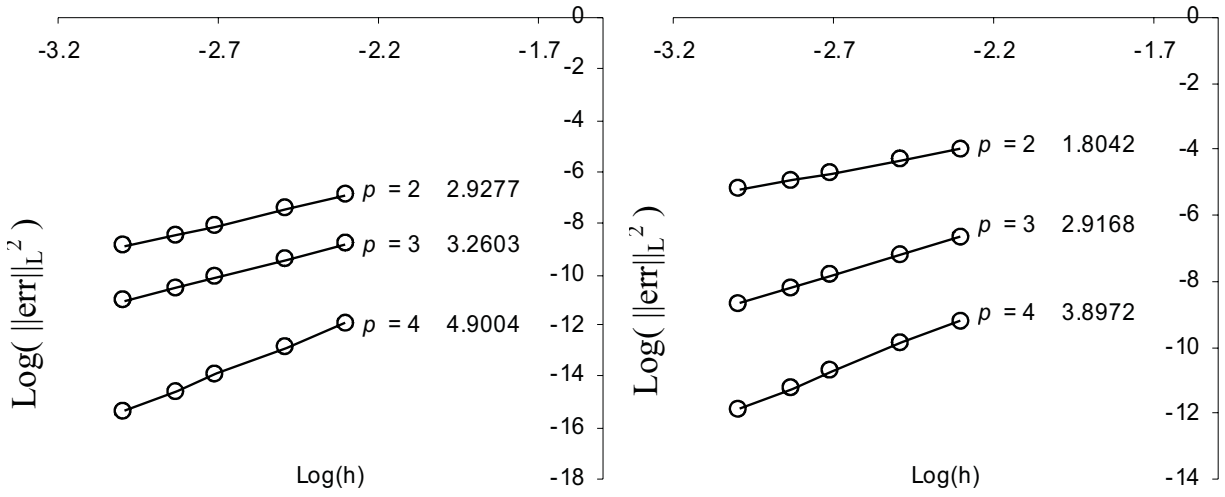

Figure 4: Error norms in one dimensional RKI approximation to (a) the exact solution; (b) first derivative of the exact solution

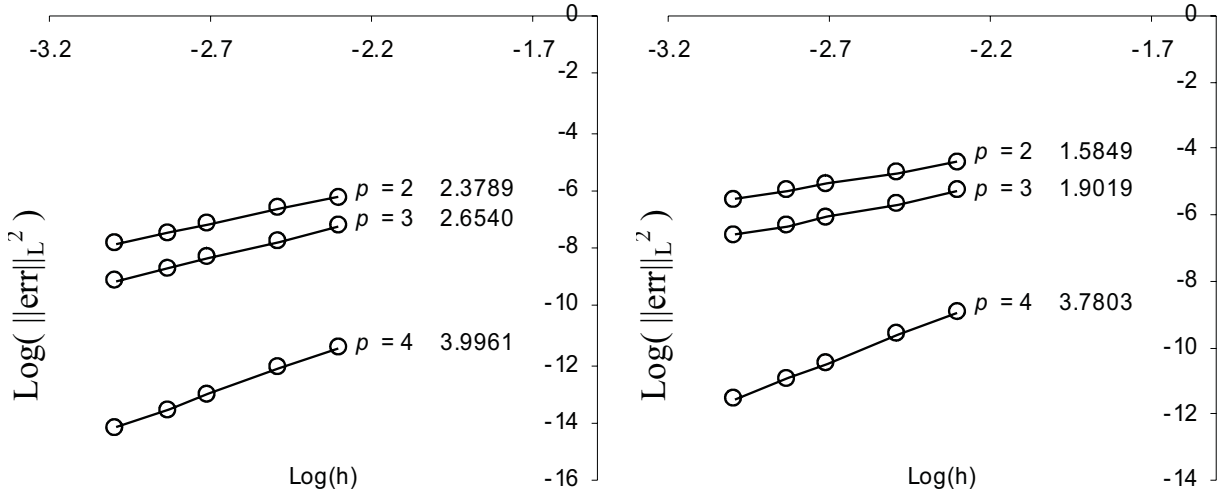

Figure 5: Error norms in one dimensional RKI collocation: (a) mesh free solution; (b) mesh free first derivatives

The above equation is subject to boundary conditions:

$$u(0) = 1; \quad u(1) = e \tag{118}$$

The exact solution is readily computable as $u(x) = e^x$. A uniform particle distribution with a constant value of the dilation parameter, $a = ((p+1)/2)\,h$, has been chosen. The above equation is solved using a collocation technique based on the new RKI scheme. Correction functions have presently been used only on the boundary nodes to get the interpolating property. Optimal order convergences for both mesh free interpolation of the known exact solution (i.e., $u(x) = e^x$) and the mesh-free numerical solution through collocation are observed. Figures (4) – (5) show the L^2 error norms of the exact and numerically obtained solutions as well as those of their first derivative for different formal orders p. The observed orders of convergence, as obtainable from

the slopes of the curves in the log-log scale are, also indicated alongside the corresponding values of the formal order.

For the second example, the following two-dimensional boundary value problem (Poisson equation) has been taken:

$$\nabla^2 u(x,y) = (x^2+y^2)e^{xy}, \quad (x,y) \in (1,0)\times(1,0) \tag{119}$$

The above equation is subjected to the following boundary conditions:

$$u(0,y) = 1, \quad u(1,y) = e^y, \quad 0 \le y \le 1 \tag{120}$$

$$u(x,0) = 1, \quad u(x,1) = e^x, \quad 0 \le x \le 1 \tag{121}$$

The exact solution of equation (119) is $u(x,y) = e^{xy}$. A uniform particle distribution with a constant dilation parameter $1.5(p+1)h/2$ has been used. Figures (6) – (7) show the L^2 error norms of the RKI interpolation of the exact solution, RKI collocation-based mesh-free solution and those of their first derivative for different formal orders p. The observed orders of convergence are also noted alongside the formal values of p. The increase in the order of convergence with increasing p is evident. It may be generally observed that a very satisfactory rate convergence is achievable through the new RKI technique.

Numerical examples

The present section is concerned with the numerical application and explorations of the proposed method for a class of nonlinear boundary value problems (BVP-s) of interest in solid mechanics. In all the examples, a mixed reproducing kernel interpolation approach (i.e., with correction functions being used only on the boundary nodes where Dirichlet boundary conditions are specified) are used unless otherwise specified. Exponential kernel function, as given in equation (46), is used to construct correction functions. Since all the numerical solutions reported below are through a collocation technique based on the new RKI discretization strategy, such solutions must be construed in the strong sense (as opposed to weak solutions, as in the variational or a weighted residual formulation).

Example 1 (Elastica)

In the first example a planar, large-deflection (Elastica) problem of a cantilever beam of length L subjected to a transverse, concentrated load, P, at its free end is considered. The governing 2^{nd} order nonlinear ODE is given by:

$$\frac{d^2\theta}{ds^2} + \lambda^2 \cos\theta = 0 \tag{122}$$

$$\text{with } \lambda^2 = \frac{P}{EI} \tag{123}$$

where, θ, P and EI are respectively the slope, lateral load and flexural rigidity of the beam and s denotes the independent spatial coordinate along the deformed longitudinal axis (deformed centroidal axis). The new RKI shape functions are constructed using cubic basis functions ($p = 3$)and uniform support size $a = 2.1\Delta x$, where Δx is the spatial step size. The new RKI-based results are compared with those via an exact method (i.e., closed-form solutions obtainable through elliptic integral) and the commercially available finite element program ANSYS®. The solutions are also compared with the regular RKPM approximation. Such comparisons are provided in Table 1. Deflected shapes of cantilever beam at different values of PL^2/EI are shown in figure (8). In figure (9), comparisons of slope (at the free end) with those obtained via elliptic integrals and RKPM (regular) have been shown for different values of the normalized load, PL^2/EI.

Example 2 (Plastica)

In this example, the elasto-plastic behaviour of a cantilever beam (figure 10) has been studied. The equation governing large plastic deformations of beams, known as the Plastica equation (Yu and Johnson 1982), may be written as:

$$\frac{d\theta}{ds} = \frac{\beta}{\sqrt{(1-2f\delta_p+2fy)}}, \quad 0 \le s \le l \tag{124}$$

$$\frac{d\theta}{ds} = \beta[1-f(y-\delta_p)], \quad l \le s \le 1 \tag{125}$$

$$\frac{dx}{ds} = \cos\theta, \quad \frac{dy}{ds} = \sin\theta \tag{126}$$

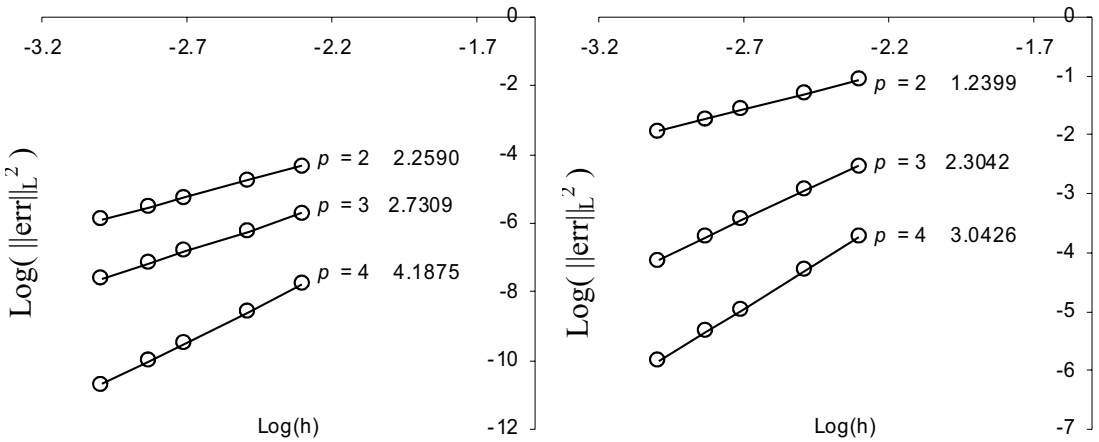

Figure 6: Error norms in two-dimensional RKI approximation to (a) the exact solution; (b) first derivatives of the exact solution

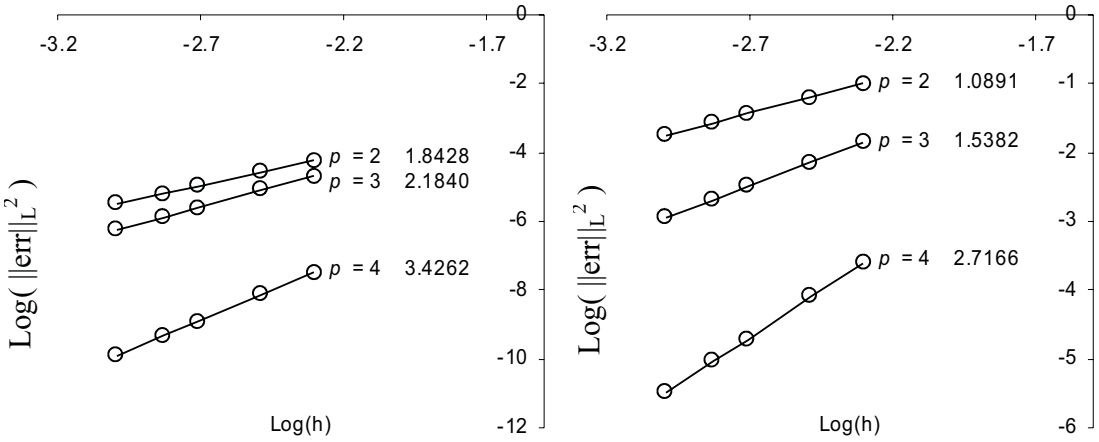

Figure 7: Error norms in two-dimensional RKI collocation (a) mesh free solution; (b) mesh free first derivatives

Table 1: Deflection and slopes of a tip loaded cantilever beam

PL^2/EI	Exact [Mattiasson 1981]			RKPM (regular)			RKI (New)		
	w/L	u/L	θ_0	w/L	u/L	θ_0	w/L	u/L	θ_0
1	0.30172	0.05643	0.46135	0.30172	0.05643	0.46136	0.30172	0.05643	0.46136
2	0.49346	0.16064	0.78175	0.49348	0.16065	0.78177	0.49348	0.16064	0.78178
3	0.60325	0.25442	0.98602	0.60329	0.25444	0.98607	0.60329	0.25443	0.98607
4	0.66996	0.32894	1.12124	0.67002	0.32898	1.12132	0.67003	0.32897	1.12133
5	0.71379	0.38763	1.21537	0.71387	0.38769	1.21548	0.71388	0.38768	1.21549
6	0.74457	0.43459	1.28370	0.74467	0.43467	1.28384	0.74469	0.43466	1.28385
7	0.76737	0.47293	1.33496	0.7675	0.47303	1.33513	0.76751	0.47302	1.33515
8	0.78498	0.50483	1.37443	0.78514	0.50496	1.37463	0.78516	0.50495	1.37465
9	0.79906	0.53182	1.40547	0.79924	0.53198	1.40569	0.79926	0.53197	1.40571
10	0.81061	0.55500	1.43029	0.81082	0.55519	1.43054	0.81085	0.55517	1.43056

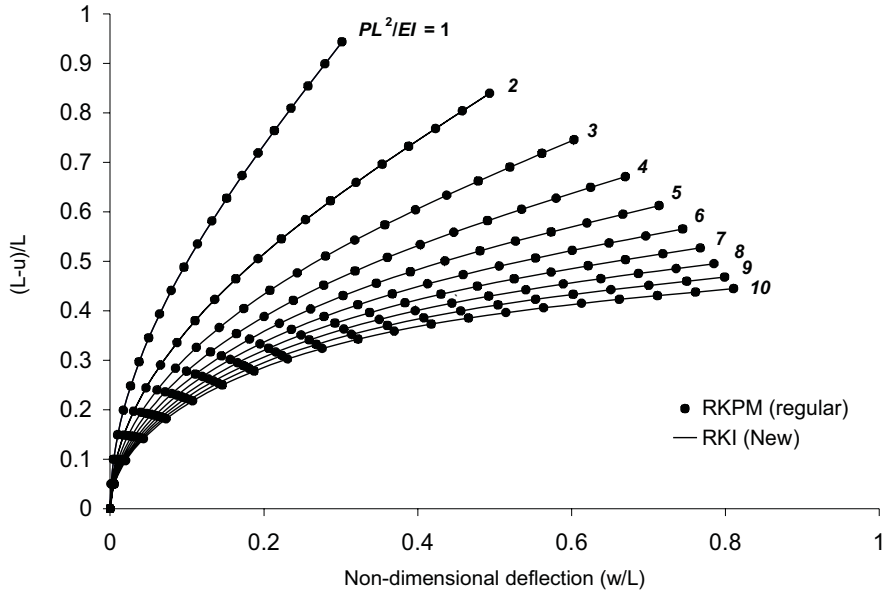

Figure 8: Deflected shapes of a cantilever Elastica (subjected to a tip load) for different values of PL^2/EI

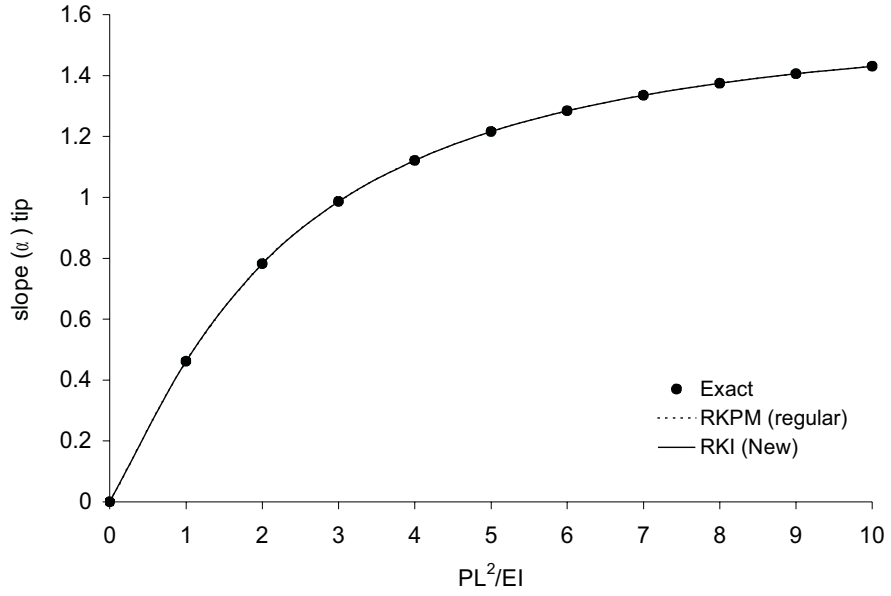

Figure 9: Variation of slope at free end with load for a cantilever beam subjected to a tip load

where, θ is the local angle of inclination, $s = s^*/L$ is the non-dimensional arc length, s^* is arc length, L_p is length of plastic region, $\beta = M_e L_p/EI$ is the non-dimensional parameter , $\delta_p = \delta_p^*/L_p = y(1)$ is the non-dimensional deflection of point C, $\delta_p^* = y^*|_{s^*=L_p}$ is the deflection of point C, $l = L_p/L$, $x = x^*/L$ and $y = y^*/L$ are non-dimensional Cartesian coordinates and $f \equiv \frac{FL_p}{M_e}$ is the non-dimensional load parameter. Boundary conditions are:

$$\theta(0) = y(0) = x(0) = 0 \tag{127}$$

$$y(1) = \delta_p \quad \text{or} \quad \theta'(1) = \beta, \quad 0 \le s \le l \tag{128}$$

where, $\theta' = \frac{d\theta}{ds}$.

Equations (124 – 126) along with boundary conditions (127, 128) lead to the following boundary value problem involving a non-linear second-

order ODE:

$$\beta^2 \frac{d^2\theta}{ds^2} = -f\left(\frac{d\theta}{ds}\right)^3 \sin\theta \tag{129}$$

with $\theta(0) = 0$ and $\theta'(1) = \beta$. Equation (129) has been solved through a collocation new RKI method. Cubic basis functions ($p = 3$) and uniform support size $a = 2.1\Delta x$ (Δx being the spatial step size) have been adopted for the construction of new RKI basis functions. The results have been compared with the results of 'exact' numerical integration for $\beta = 0.1$ in Table 3. Results obtained by the proposed method are very close to the 'exact' results.

Example 3 (von Karman plate)

Finally, a non-linear plate bending problem is studied using the new method and the results are compared with those already documented in the literature. Unlike the last two examples, the present example has up to fourth order derivatives in the governing differential equations. The nonlinear von Karman PDE-s governing the static equilibrium of a thin plate in the absence of body forces may be written in terms of displacement functions as (Chia 1980):

$$u_{,xx} + d_1 u_{,yy} + d_2 v_{,xy} + w_{,x}(w_{,xx} + d_1 w_{,yy}) + d_2 w_{,y} w_{,xy} = 0 \tag{130}$$

$$v_{,xx} + d_1 v_{,xx} + d_2 u_{,xy} + w_{,y}(w_{,yy} + d_1 w_{,xx}) + d_2 w_{,x} w_{,xy} = 0 \tag{131}$$

$$\nabla^4 w - \frac{Eh}{D(1-\mu^2)}\Big[\left(u_{,x} + 0.5w_{,x}^2\right)\left(w_{,xx} + \mu w_{,yy}\right) + \left(v_{,y} + 0.5w_{,y}^2\right)\left(w_{,yy} + \mu w_{,xx}\right) + (1-\mu) w_{,xy}\left(u_{,y} + v_{,x} + w_{,x} w_{,y}\right)\Big] = \frac{q}{D} \tag{132}$$

where, $\nabla^4 w = w_{xxxx} + 2w_{xxyy} + w_{,yyyy}$ and, $d_1 = \frac{1-\mu}{2}$, $d_2 = \frac{1+\mu}{2}$, $D = \frac{Eh^3}{12(1-\mu^2)}$

For a simply supported rectangular plate, the boundary conditions are:

$u = v = w = 0$ at $x = \pm\frac{a}{2}$; $u = v = w = 0$ at $y = \pm\frac{b}{2}$

In the above equations, μ, E and h respectively denote the Poisson's ratio, the modulus of elasticity and the thickness of the plate. u, v, w are the displacement functions in X, Y, Z directions respectively and q denotes a uniformly distributed lateral load. The parameters a and b are lengths of the two sides of the rectangular plate.

The plate is discretized with $11 \times 11 = 121$ nodes as shown in figure 11. Shape functions (regular RKPM and new RKI) have been constructed with $p = 4$ and a uniform support size with $a_x = 3.15\Delta x$ and $a_y = 3.15\Delta y$ (Δx, Δy are the spatial step sizes and a_x, a_y are the dilation parameters in X and Y directions respectively). The transverse displacement w at the centre is obtained via the new RKI method for various intensities of uniformly distributed lateral load and the results are compared with those of Levy (1942), ANSYS® and RKPM (regular). The nonlinear elastic load-deflection curve at the center of the plate is shown in figure 12. While results via the new RKI and regular RKPM schemes match very well with Levy's solutions, results via ANSYS® are a little off especially for higher values of the loading intensity. Figure 13 reports the convergence of the central transverse deflection with increasing number of particles (nodes) as obtained via different methods. The new RKI method not only appears to have the fastest convergence, it is also seen to be predicting the response more accurately. As has been already noted, computations of derivatives in regular RKPM and RKI (Chen *et al.*) may potentially lead to considerable numerical error especially when spatial step size is very small. Moreover in the interpolating version of RKPM proposed by Chen *et al.*, primitive function had to attain its maximum value of unity (for interpolation purposes) over a typically small support size and this could very well result in an ill conditioning of the algorithm for small spatial step sizes. To demonstrate the effect (sensitivity) of spatial step sizes on various methods, the von Karman plate equation (132) is now solved with $21 \times 21 = 441$ nodes using $a_x = 3.15\Delta x$ and $a_y = 3.15\Delta y$. Figure 14 shows the normalized central transverse deflection as a function of the normalized load intensity via different methods. It is clear that,

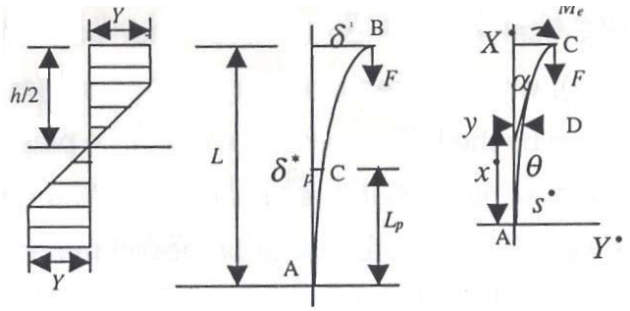

Figure 10: (a) The elastic-plastic stress distribution across a section; (b) A vertical strut loaded by a vertical force at its free end; (c) A vertical strut loaded by the maximum elastic bending moment and a vertical force at its free end

Table 2: slope (α) and deflection (δ) at the free end of the cantilever beam

f=FL/M_e	Exact	RKPM (regular)	RKI (New)	=FL/M_e	Exact	RKPM (regular)	RKI (New)
0	0.10000	0.10000	0.10000	0	0.04999	0.04996	0.04996
1	0.10371	0.10370	0.10370	1	0.05231	0.05228	0.05228
2	0.10850	0.10843	0.10843	2	0.05537	0.05530	0.05530
3	0.11531	0.11503	0.11503	3	0.05982	0.05959	0.05958
4	0.12775	0.12772	0.12771	4	0.06823	0.06818	0.06818
4.4	0.14124	0.14110	0.14110	4.4	0.07779	0.07770	0.07772

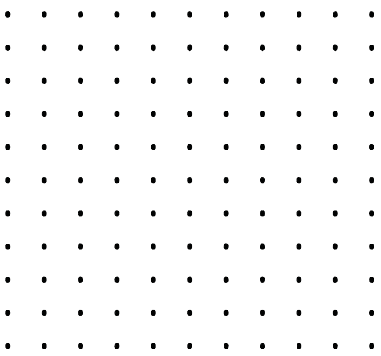

Figure 11: Domain discretization with 121 nodes

even with very small spatial and support sizes, new RKI works very well, whereas RKPM (regular) and RKI (Chen *et al.*) converge to wrong solutions.

8 Concluding Remarks

A novel form of mesh-free and interpolating functional approximations and accurate computations of derivatives is proposed based on the reproducing kernel approach. In the conventional RKPM approach, it is required to differentiate the moment matrix and correction functions so as to compute derivatives of shape functions. Such an exercise is potentially fraught with the danger of being numerically error-prone especially in higher order derivatives. This difficulty is presently overcome through a novel scheme for computing derivatives of RKPM basis functions. The scheme is based on the principle that α^{th} derivative of RKPM basis functions will exactly reproduce the α^{th} derivative of space of polynomial P_p of degree $p \geq |\alpha|$. This derivate reproduction scheme does not require differentiations of moment matrices and correction functions. More-

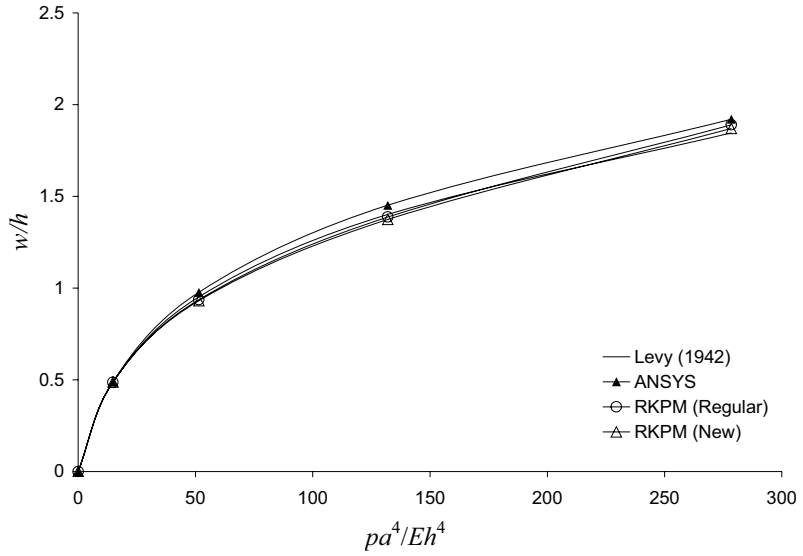

Figure 12: Variation of central transverse deflection with load for a simply supported isotropic square plate

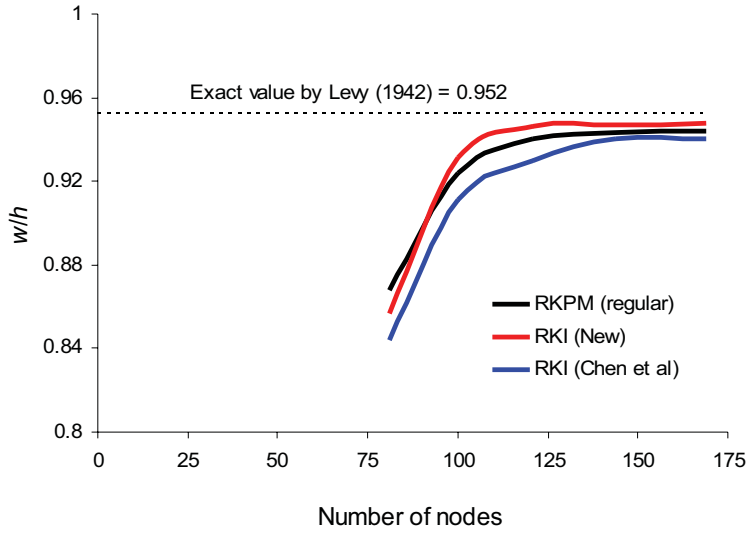

Figure 13: Convergence of central deflection at $pa^4/Eh^4 = 51.4$ with number of points

over, the novelty of the interpolating mesh-free scheme, proposed in this study, is based upon a linear combination of two distinct families of RK basis functions. The use of B-spline functions to construct one of these families of basis functions helps bring in the local support property in a seamless manner. As evidenced through derivations of the new RKI shape functions as well as through limited numerical experimentations conducted on a few test cases, the current version of mesh-free interpolation strategy provides a more accurate and stable computational framework than an earlier strategy by Chen *et al.* (2003). These last authors introduced the concept of a primitive function to bring in the Kronecker delta properties in the approximation. The approximation consisted of a summation of primitive and reproducing kernel (enrichment) functions and required the support size of the primitive function to be less than the smallest distance between two successive grid points over which the enrichment functions were defined. Accordingly, the primitive function had to attain its maximum value of unity (for interpolation purposes) over

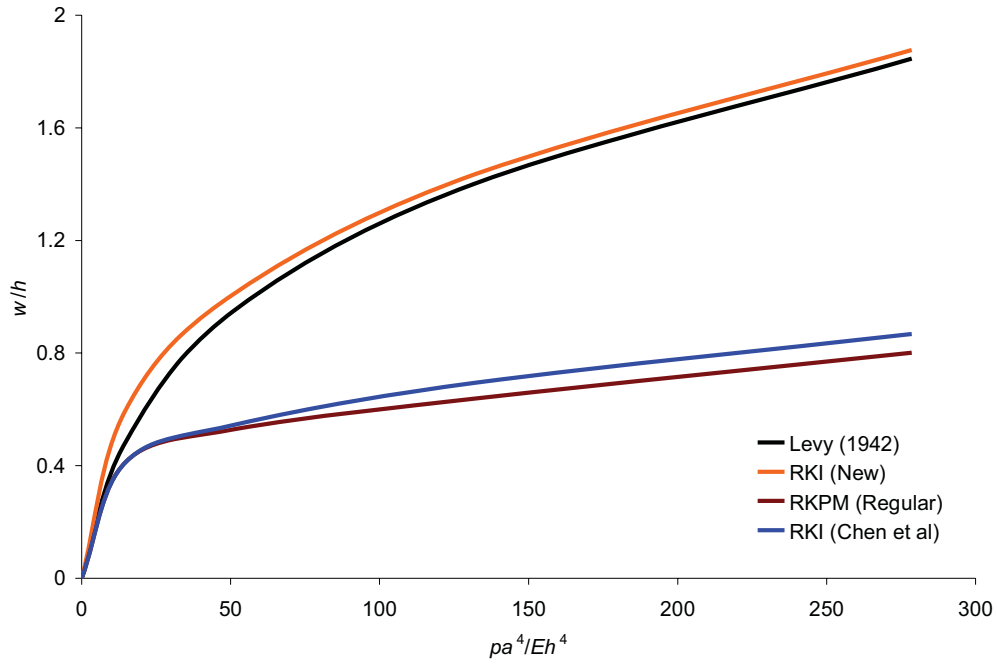

Figure 14: Variation of central transverse deflection with load for a simply supported isotropic square plate with $21 \times 21 = 441$ nodes and $a_x = 3.15\Delta x$ and $a_y = 3.15\Delta y$

a typically small support size and this led to an ill conditioning of the algorithm. In contrast, the present interpolating method determines the coefficients of a linear combination of a couple of distinct families of RK shape functions via the interpolating conditions. In the process, the twin objectives of polynomial reproduction and interpolation are together met by the two families of basis functions and thus, unlike the approach by Chen *et al*. (2003), none of these two families of functions has to separately satisfy the Kronecker delta property and there are no imposed restrictions on the support sizes.

A major usefulness of a mesh-free method is the flexibility with which the nodal points can be re-adjusted to accurately capture zones of sharp gradient changes or different length scales (as in problems with localized plastic zones). A natural framework to derive a numerical scheme for obtaining strong solutions of such problems is to use a mesh-free wavelet collocation technique. Towards this, the presently developed mesh-free shape functions may be exploited to arrive at a suitable nesting of wavelet subspaces. In addition, such schemes are expected to be ideally suitable if the mechanics of the problem is modeled with Cosserat theories which have length scales naturally built into them. The authors are now in the process of addressing some of these issues.

Reference

Aluru N.R. (2000): A point collocation method based on reproducing kernel approximations. International Journal for Numerical Methods in Engineering; Vol. 47, pp. 1083 –1121.

Atluri, S. N. (2005): "Methods of Computer Modeling in Engineering & the Sciences-Part I", 480 pages, Tech Science Press.

Atluri, S. N. (2004a): "The Meshless Method(MLPG) for Domain & BIE Discretizations, 680 pages, Tech Science Press.

Atluri S. N., Han Z. D., Rajendran A. M. (2004b): "A new implementation of the meshless finite volume method, through the MLPG "Mixed" approach", *CMES:Computer Modeling in Engineering & Sciences*, 6(6), pp. 491-513.

Atluri S. N., Liu H. T., and Han Z. D. (2006a):

"Meshless Local Petrov-Galerkin (MLPG) Mixed Finite Difference Method for Solid Mechanics", *CMES: Computer Modeling in Engineering & Sciences*, 15(1), pp.1-16.

Atluri S.N., Kim H.G., Cho JY. (1999): A critical assessment of the truly Meshless local Petrov–Galerkin (MLPG) methods. *Computational Mechanics*, Vol. 24, pp. 348–372.

Atluri S. N., Liu H. T., and Han Z. D. (2006b): "Meshless Local Petrov-Galerkin(MLPG) Mixed Collocation Method for Elasticity Problems", *CMES: Computer Modeling in Engineering & Sciences*, 14(3), pp.141-152.

Atluri, S. N., and Shen, S. (2002a): "The Meshless Local Petrov-Galerkin (MLPG) Method", 440 pages, Tech Science Press.

Atluri S. N., Shen S. P. (2002b): "The meshless local Petrov-Galerkin (MLPG) method: A simple & less-costly alternative to the finite element and boundary element methods" *CMES: Computer Modeling in Engineering and Sciences*, 3 (1), pp. 11-51

Atluri, S. N., and Zhu, T. (1998): "A New Meshless Local Petrov-Galerkin (MLPG) Approach in Computational Mechanics", *Computational Mechanics*, Vol.22, pp. 117-127.

Au, C. K. and Yuen, M.M.F. (1995): Unified approach to NURBS curve shape modification, *Computer-Aided Design*, 27, 85-93.

Babuska, I. and Melenk, J. M. (1997): The partition of unity method. *International Journal of Numerical Methods in Engineering*; Vol. 40, pp. 727-758.

Barry W., Saigal S. (1999): A three-dimensional element-free Galerkin elastic and elasto-plastic formulation. *International Journal for Numerical Methods in Engineering*; Vol. 46, pp. 671–693.

Belytschko, T.; Lu Y. Y.; Gu, L. (1994): "Element-free Galerkin methods," *Int. J. Numer. Meth. Eng.*, 37, pp. 229-256

Brenner, S. C. and Scott, L. R. (1994): "The Mathematical Theory of Finite Element Methods", Springer, New York

Butterfield, K.R. (1976): "The computation of all the derivatives of a B-spline basis", *Journal of Inst. Math. Applic.*, Vol 17, pp. 15 - 25

Chen, J. S., Han, W., You, Y., Meng, X. (2003): "Reproducing kernel method with nodal interpolation property," *International Journal for Numerical Methods in Engineering*, 56, pp. 935-960

Chen, J S, Pan, C, Wu T. C., Liu, W K (1996): "Reproducing Kernel Particle Methods for large deformation analysis of non-linear structures," Comput. *Methods Appl. Mech. Engrg.*, Vol. 139, pp. 195-227

Chen J. S., Pan C., Wu T. C. (1997): "Large deformation analysis of rubber based on a reproducing kernel particle method," *Computational mechanics*; Vol. 19, pp. 211 - 227

Chia, C. Y. (1980): "Nonlinear analsis of plates", McGraw-Hill, New York.

Cox, M. G. (1972): "The numerical evaluation of B-splines, *Jour. Inst. Math. Applic.*, Vol 10, pp. 134 - 149.

De Boor, C. (1972): "On calculating with B-splines", *Jour. Approx. Theory*, Vol 6, pp. 50 - 62.

Duarte CA, Oden J T. (1997): "An h-p adaptive method using clouds," *Computer Methods in Applied Mechanics and Engineering*, Vol. 139, pp. 237-262.

Gingold RA, Monaghan JJ. (1977): "Smoothed particle hydrodynamics: theory and application to non-spherical stars," *Monthly Notices of the Royal Astronomical Society*; Vol. 181, pp. 275-389.

Gu, Y. T. and Liu, G. R. (2001a): "A boundary point interpolation method (BPIM) using radial function basis," First MIT Conference on Computational Fluid and Solid Mechanics, MIT, pp. 1590 - 1592.

Gu, Y. T. and Liu, G. R. (2001b): "A boundary point interpolation method for stress analysis of solids," *Computational Mechanics*, Vol. 28(1), pp. 47 - 54.

Han Z. D., Liu H. T., Rajendran A. M. and Atluri S. N. (2006): "The Applications of Meshless Local Petrov-Galerkin (MLPG) Approaches in High-Speed Impact, Penetration and Perforation Problems", *CMES:Computer Modeling in Engineering & Sciences*, 14(2) pp. 119-128.

Han, W. and Meng, X. (2001): Error analysis of the reproducing kernel particle method. *Computer Methods in Applied Mechanics and Engineering*, Vol. 190, pp. 6157-6181.

Han Z.D., Rajendran A. M., Atluri S. N. (2005): "Meshless Local Petrov-Galerkin (MLPG) approaches for solving nonlinear problems with large deformations and rotations", *CMES:Computer Modeling in Engineering & Sciences*, 10 (1), pp. 1-12.

Huerta A, Fernandez-Mendez S. (2000): "Enrichment and coupling of the finite element and meshless methods," International Journal for Numerical Methods in Engineering, 48, pp. 1615 - 1636.

Kaljevic I, Saigal S. (1997) An improved element-free Galerkin method. *International Journal for Numerical Methods in Engineering*; Vol. 40, pp. 2953-2974.

Krongauz Y, Belytschko T. (1996) "Enforcement of essential boundary conditions in meshless approximations using finite elements," *Computer Methods in Applied Mechanics and Engineering*, Vol. 131, pp. 133 -145

Levy, S. (1942): "Bending of rectangular plate with large deflection", NACA Report No. 737, pp. 139 - 157

Li, S., Lu, H., Han, W. and Liu., W. K. (2004): "Reproducing Kernel Element Method, Part II Globally Conforming Im/Cn Hierarchies," Computer Methods in Applied Mechanics and Engineering, 193, pp. 953 - 987

Liu, G. R. and Gu, Y. T. (1999): "A point interpolation method," Proc. 4th Asia-Pacific Conference on computational Mechanics, Singapore, pp. 1009 - 1014.

Liu, G. R. and Gu, Y. T. (2000b): "Vibration analysis of 2-D solids by the local point interpolation method (LPIM), Proc. 1st International Conference on Structural Stability and Dynamics, Taiwan, pp. 411 - 416.

Liu, G. R. and Gu, Y. T. (2000d): "Coupling of element free Galerkin method with boundary point interpolation method," *Advances in computational Engineering and Science*, Atluri, S. N. and Brust, F. W., Eds., ICCES'2K, Los Angeles, pp. 1427 - 1432.

Liu, G. R. and Gu, Y. T. (2001a): "A local point interpolation method for stress analysis of two-dimensional solids," *Strut. Eng. Mech.*, Vol. 11(2), pp. 221 - 236.

Liu, G. R. and Gu, Y. T. (2001b): "A local radial point interpolation method (LR-PIM) for free vibration analysis of 2-D solids," *J. Sound Vib.*, Vol. 246(1), pp. 29 - 46.

Liu, G. R. and Gu, Y. T. (2001c): "A point interpolation method for two-dimensional solids," *International Journal for Numerical Methods in Engineering*, Vol. 50, pp. 937 - 951.

Liu, G. R. and Gu, Y. T. (2001d): "A matrix triangularization algorithm for point interpolation method," Proc. Asia-Pacific Vibration Conference, Bangchum, W. Ed., Hangzhou, China, pp. 1151 - 1154.

Liu, W. K., Han, W., Lu, H. and Li., S. (2004): "Reproducing Kernel Element Method, Part I Theoretical Formulation," *Computer Methods in Applied Mechanics and Engineering*, 193, pp. 933 - 951

Liu W. K., Jun S, Li S, Adee J, Belytschko T. (1995b): "Reproducing kernel particle methods for structural dynamics," *International Journal for Numerical Methods in Engineering*, Vol. 38, pp. 1655 -1679.

Liu WK, Jun S, Zhang Y. F. (1995a): "Reproducing kernel particle methods," *International Journal for Numerical Methods in Fluids*, Vol. 20, pp. 1081-1106.

Liu WK, Li S, Belytschko T. (1997): "Moving least square reproducing kernel methods (I) methodology and convergence," *Computer Methods in Applied Mechanics and Engineering*, Vol. 143, pp. 422- 433

Lu, H., Li, S., Simkins, D. C., Liu, W. K., and Cao, J. (2004): "Reproducing Kernel Element Method Part III. Generalized Enrichment and Applications," *Computer Methods in Applied Mechanics and Engineering*, 193, pp. 989 - 1011

Lu YY, Belytschko T, Gu L. (1994): "A new implementation of the element free Galerkin method," *Computer Methods in Applied Mechan-*

ics and Engineering, Vol. 113, pp. 397-414.

Mattiasson K. (1981): "Numerical results from large deflection beam and frame problems analyzed by means of elliptic integrals", *Int. J. Numer. Methods Engng.*, Vol. 17, pp.145-153

Melenk J M, Babuska I. (1996): "The partition of unity finite element method: basic theory and applications," *Computer Methods in Applied Mechanics and Engineering*, Vol. 139, pp. 289-314.

Piegl, L. and Tiller, W. (1995): The NURBS Book, Springer, Berlin.

Simkins, D.C., Li, S., Lu, H. and Liu, W. K. (2004): "Reproducing Kernel Element Method Part IV. Globally Conforming Cn(n 1) Triangular Hierarchy," *Computer Methods in Applied Mechanics and Engineering*, 193, pp. 1013 - 1034

Wagner G. J., Liu W. K. (2001): "Hierarchical enrichment for bridging scales and meshfree boundary conditions," *International Journal for Numerical Methods in Engineering*, Vol. 50, pp. 507-524

X. Jin, G. Li and N. R. Aluru (2001): "On the equivalence between least-squares and kernel approximations in meshless methods", *CMES: Computer Modeling in engineering and Sciences*, Vol. 2, No. 4, pp. 447-462,

Yu, T.X., Johnson, W. (1982): "The Plastica: the large elastic-plastic deflection of a strut", *Int. J. Non-Linear Mech.*, Vol.17, pp.195-209

Zhu T, Zhang J, Atluri SN. (1998): "A meshless local boundary integral equation (LBIE) method for solving nonlinear problems," *Computational Mechanics*, Vol. 22, pp. 174 -186

Appendix A

A.1 B-spline basis functions

B-spline curves are generalization of Bézier curves. The recursive definition (deBoor 1972 and Cox 1972) of the i^{th} normalized B-spline basis functions of degree p (order $p+1$) is

$$N_{i,0}(\xi) = \begin{cases} 1 & \text{if } \xi_i \le \xi \le \xi_{i+1} \\ 0 & \text{otherwise} \end{cases} \tag{A.1}$$

$$N_{i,p}(\xi) = \frac{\xi - \xi_i}{\xi_{i+1} - \xi_i} N_{i,p-1}(\xi) + \frac{\xi_{i+p+1} - \xi}{\xi_{i+p+1} - \xi_{i+1}} N_{i+1,p-1}(\xi), \quad i = 1,2,3,\ldots\ldots n+p+1 \tag{A.2}$$

where, $\Xi = \{\xi_1, \xi_2, \xi_3 \ldots\ldots \xi_{n+p+1} | \xi_i \in R\}$ is a non-decreasing sequence of real numbers called knot vector, p is the polynomial order and n is the number of basis functions. In the above definition it is assumed that 0/0 is replaced by 0. If knots are equally spaced they are called uniform. Knots can be repeated at the same coordinate in the parametric space. A knot vector is said to be open if its first and last knot appear $p+1$ times. Basis functions in one dimension formed from the open knot vector are interpolatory at the ends of the parametric space$\Xi = \left[\xi_1,\ \xi_{k+p+1}\right]$. Although $N_{i,p}(\xi)$ is defined everywhere on the real line, it has non-zero values only in the interval $[\xi_i, \xi_{i+p+1}]$ because of its local support property. An example of cubic basis function for a uniform knot vector (open and closed) is presented in figure A.1.

Derivatives of B-spline basis functions

The k^{th} derivative of B-spline basis functions in terms of the functions $N_{i,p-k}, \ldots, N_{i+k,p-k}$ is given by:

$$N_{i,p}^{(k)} = \frac{p!}{(p-k)!} \sum_{j=0}^{k} a_{k,j} N_{i+j,p-k} \tag{A.3}$$

with

$$a_{0,0} = 1 \tag{A.4}$$

$$a_{k,0} = \frac{a_{k-1,0}}{\xi_{i+p-k+1} + \xi_i} \tag{A.5}$$

$$a_{k,j} = \frac{a_{k-1,j} - a_{k-1,j-1}}{\xi_{i+p+j-k+1} + \xi_{i+j}}, \quad j = 1, \ldots, k-1 \tag{A.6}$$

$$a_{k,k} = \frac{-a_{k-1,k-1}}{\xi_{i+p+1} + \xi_{i+k}} \tag{A.7}$$

Note that the denominators involving knot differences can became zero; the quotient is defined to be zero in this case. The k^{th} derivative of B-spline

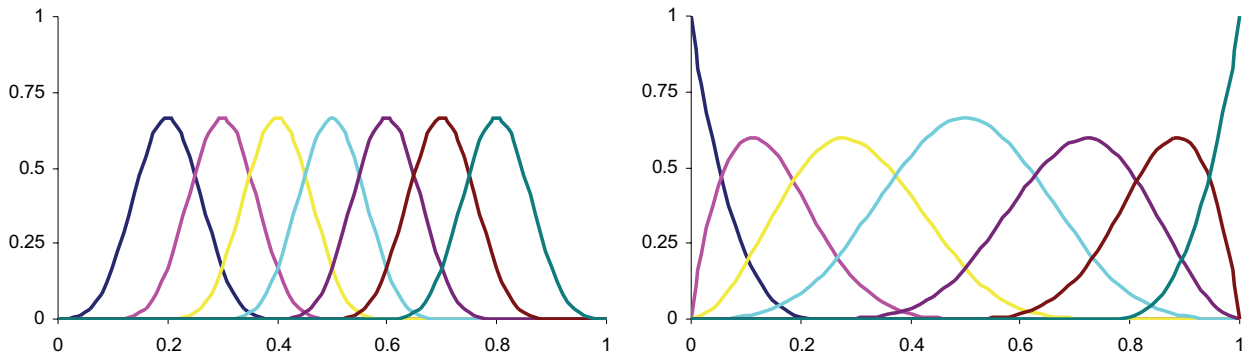

Figure A.1: Cubic B-spline basis function for (a) uniform knot vector Ξ ={0, 0.1, 0.2, 0.3, 0.4, 0.5, 0.6, 0.7, 0.8, 0.9, 1.0} (b) open uniform knot vector Ξ ={0, 0, 0, 0, 0.25, 0.5, 0.75, 1.0, 1.0, 1.0, 1.0}

basis functions may also be computed as (Butterfield, K. R. 1976):

$$N_{i,p}^{(k)}(\xi) = \frac{p}{p-k} \cdot \left(\frac{\xi - \xi_i}{\xi_{i+1} - \xi_i} N_{i,p-1}^{(k)}(\xi) + \frac{\xi_{i+p+1} - \xi}{\xi_{i+p+1} - \xi_{i+1}} N_{i+1,p-1}^{(k)}(\xi) \right) \quad k = 0, \ldots, p-1 \quad \text{(A.8)}$$

Some important properties of B-spline basis functions:

(1) **The local support property:** $N_{i,p}(\xi) = 0$ if ξ is outside the interval $[\xi_i, \xi_{i+p+1})$.

(2) In any given knot span, $[\xi_i, \xi_{i+1})$, at most $p+1$ of $N_{i,p}(\xi)$ are nonzero, namely the functions $N_{j-p,p}, \ldots, N_{j,p}$. For example, the only cubic functions not zero on $[\xi_3, \xi_4)$ are $N_{0,3}, \ldots, N_{3,3}$.

(3) **Non-negativity:** $N_{i,p}(\xi) \geq 0, \forall i, p, \xi$.

(4) **Partition of unity:** For an arbitrary knot span $[\xi_i, \xi_{i+1})$, one has $\sum_{j=i-p}^{i} N_{j,p}(\xi) = 1, \ \forall \xi \in [\xi_i, \xi_{i+1})$.

(5) All derivatives of $N_{i,p}(\xi)$ exist in the interior of a knot span. At a knot, $N_{i,p}(\xi)$ is $p-k$ times continuously differentiable, where k is the multiplicity of the knot. Hence, increasing the degree increases continuity, and increasing knot multiplicity decreases continuity.

(6) Except for the case $p = 0$, $N_{i,p}(\xi)$ attains exactly one maximum value.

A.2 B-spline curves

Using the B-spline basis function discussed in section A.1, B-spline curves may be constructed as:

$$C(\xi) = \sum_{i=1}^{n} N_{i,p}(\xi) P_i \quad \text{(A.9)}$$

where, P_i are the coefficients of B-spline basis function and called control points. In general control points are not interpolated by B-spline curves. It defines the shape of the curves and t he polygon formed by $\{P_i\}$ is called the control polygon. An example of cubic B-spline curve on a open uniform knot is shown in figure A.2.

A.2.1 Derivatives of B-spline curves

Derivatives of B-spline curve may be computed according to the following rule.

(1) When ξ is fixed:

$$C^{(k)}(\xi) = \sum_{i=1}^{N_p} N_{i,p}^{(k)}(\xi) P_i \quad \text{(A.10)}$$

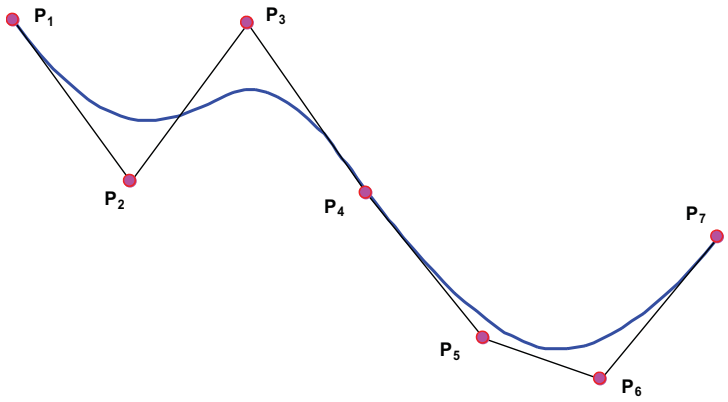

Figure A.2: Cubic B-spline curve on an open uniform knot vector Ξ ={0, 0, 0, 0, 0.25, 0.5, 0.75, 1.0, 1.0, 1.0, 1.0}, basis functions are shown in figure A.1 (b)

where, $C^{(k)}(\xi)$ and $N_{i,p}^{(k)}(\xi)$ denote the k^{th} derivative of $C(\xi)$ and $N_{i,p}(\xi)$ respectively. $N_{i,p}^{(k)}(\xi)$ may be computed as discussed in section A.1.1.

(2) When ξ is not fixed:
Without fixing ξ, adversatives of p^{th} degree B-spline curve may be computed as:

$$C^{(k)}(\xi) = \sum_{i=1}^{n-k} N_{i,p-k}(\xi) P_i^{(k)} \tag{A.11}$$

with

$$P_i^{(k)} = \begin{cases} P_i & k = 0 \\ \frac{p-k+1}{\xi_{i+p+1} - \xi_{i+k}} (P_i^{(k-1)} - P_i^{(k-1)}) & k > 0 \end{cases} \tag{A.12}$$

and

$$\Xi^{(k)} = \{0, \ldots 0, \xi_{p+1}, \ldots \xi_n, 1, \ldots 1\} \tag{A.13}$$

A few important properties of B-spline curves are as indicated below.

(1) They have continuous derivatives of order p – k, where k is multiplicity of knot. Hence in the absence of any repeated knot or control points it is $p-1$ times continuously differentiable.

(2) **Affine invariance:** any affine transformation can be obtained by applying the transformation to the control points.

(3) **Strong convex hull property:** the curve is contained in the convex hull of its control polygon

(4) **Variation diminishing property:** no straight line intersects the curve more times than it intersects the curve's control polygon. This expresses the property that a B-spline curve follows its control polygon rather closely and does not wiggle more than its control polygon.

A.3 B-splines in higher dimension

Higher dimensional B-spline basis function may be constructed by taking the tensor product of B-spline basis function in one dimension.

A.3.1 B-spline surface

A B-spline surface is obtained by taking a bidirectional net of control points, two knot vectors and the products of the univariate B-spline function

$$S(\xi, \eta) = \sum_{i=1}^{N_{P\xi}} \sum_{j=1}^{N_{P\eta}} N_{i,p}(\xi) N_{j,q}(\eta) P_{ij} \tag{A.14}$$

where $N_{i,p}(\xi)$ and $N_{j,q}(\eta)$ are two different set of one dimensional B-spline basis function of order p and q and defined on the knot vectors $\Xi = \{\xi_1, \xi_2, \xi_3 \ldots\ldots \xi_{n+p+1} | \xi_i \in R\}$ and $\overline{\Xi} = \{\eta_1, \eta_2, \eta_3 \ldots\ldots \eta_{n+q+1} | \eta_i \in R\}$ respectively. Noting that $\{P_{ij}\}$, $i = 1, 2, \ldots N_{P\xi}$, $j = 1, 2, \ldots N_{P\eta}$ is the control net.

A.3.2 B-spline solids

B-spline solids are defined in analogous fashion to B-spline surfaces. Given a control net $\{P_{ijk}\}$, $i = 1,2,...N_{P\xi}$, $j = 1,2,\ldots N_{P\eta}$, $j = 1,2,\ldots N_{P\varsigma}$ and knot vectors $\Xi = \{\xi_1,\xi_2,\xi_3\ldots\xi_{n+p+1}|\xi_i \in R\}$, $\overline{\Xi} = \left\{\eta_1,\eta_2,\eta_3\ldots\ldots\eta_{n+q+1}|\eta_i \in R\right\}$ and $\tilde{\Xi} = \{\varsigma_1,\varsigma_2,\varsigma_3\ldots\ldots\varsigma_{n+r+1}|\varsigma_i \in R\}$, a B-spline solid is defined as:

$$S(\xi,\eta,\varsigma) = \sum_{i=1}^{N_{P\xi}}\sum_{j=1}^{N_{P\eta}}\sum_{k=1}^{N_{P\varsigma}} N_{i,p}(\xi)N_{j,q}(\eta)N_{j,r}(\varsigma)P_{ijk} \tag{A.15}$$